1979

Design of a Vertical Axis and Turbine-variable Speed Heat Pump Alternate Energy System

John V. Karnitis

DESIGN OF A VERTICAL AXIS WIND TURBINE-VARIABLE SPEED HEAT PUMP ALTERNATE ENERGY SYSTEM

BY

JOHN V. KARNITIS

A thesis submitted
in partial fulfillment of the requirements for the
degree Master of Science, Major in
Agricultural Engineering
South Dakota State University

1979

DESIGN OF A VERTICAL AXIS WIND TURBINE-VARIABLE SPEED HEAT PUMP ALTERNATE ENERGY SYSTEM

This thesis is approved as a creditable and independent investigation by a candidate for the degree, Master of Science, and is acceptable for meeting the thesis requirements for this degree. Acceptance of this thesis does not imply that the conclusions reached by the candidate are necessarily the conclusions of the major department.

Thesis Advisor Date

Head of Major Department Date

TABLE OF CONTENTS

TABLE OF FIGURES

LIST OF TABLES

INTRODUCTION

Energy use in agriculture is increasing with greater demands for increased productivity, and during the same period, nonrenewable energy sources such as fossil fuels are becoming more expensive and less available. Power generated from wind offers one alternate solution for decreasing the fossil fuel demand in the agricultural sector.

In many areas of the United States, particularly in the Great Plains, winds have velocities that can produce useful amounts of energy, Blackwell and Feltz (11), Reed (42). East Central South Dakota, which is a part of the Great Plains area, also has substantial amounts of energy available from the wind, Verma (55).

Wind energy use has been exploited in the past for transportation and for industrial, and consumer applications, but with the availability of inexpensive and plentiful fossil fuel it has not been widely utilized. Presently, due to energy shortages, there is a renewed interest in the wind as a potential source of energy, Primary emphasis, for the utilization of wind energy, has been on large scale commercial production of electrical energy through the use of generators of 50 kilowatts or larger, Banas and Sullivan (8), Golding (25), Swift, Jr. (51), Maile (37), Thresher and Wilson (54). Small 2 to 50 kw wind energy plants installed on individual farmsteads, however, are a potential source of energy for rural areas, Clark and Schneider (19), Cummings (21), Gunkel and Furry (26), Simonds and Bodek (46), and Soderholm (47).

The variability and discontinuity of the wind are difficulties which are associated with the utilization of wind energy for continuous

power production. Even in very windy areas there is no certainty, that the wind will blow at a particular time and with a given force. Therefore, a single wind energy source is not suitable for continuous power production unless methods are used to store the delivered wind energy, during periods of low wind and periods of no wind. Wind energy can also provide a supplemental source of energy for applications that do not need continuous power or that have a backup energy source available.

Many types of wind turbine designs have been utilized, but generally the wind machines can be divided into two basic categories. One category is the vertical-axis wind turbines and the other is the horizontal axis wind machine. The vertical axis wind turbines, which include the Darrieus and the Savonius rotors, are not as widely known as the horizontal wind rotors, but exhibit several advantages over the horizontal axis windmills. The primary benefits include the acceptance of wind from any direction, thus excluding the necessity for the yaw mechanisms, and the location of the power takeoffs at the ground level for convenient maintenance.

Most vertical axis wind turbine energy conversion systems utilize the cable tie-down system as compared to the cantilevered, unguyed system, Banas and Sullivan (8), South and Rangi (48), Templin (52), Clark and Schneider (19), Simonds and Bodek (46), Chasteau (16), Maile (37), and Hagen (27). The cable tie-down system is described by having the turbine rotor and mast supported by several guy cables which are connected from the ground locations to a point at the top of the turbine rotor.

A simple and less complex vertical axis wind energy conversion

system can be designed by utilizing the cantilevered unguyed principle, in conjunction with a compound turbine rotor consisting of Savonius and three-bladed Darrieus rotors, which has the potential for minimal vibration problems. For a cable tie-down system, the interplay, between the tower, guy wire, blade, and rotor natural frequencies, has to be properly integrated to minimize the resonant conditions. Since there is no need to pre-tension the guy cables for an unguyed system, there is also no need for cable anchors and tensioning mechanisms, thus savings in materials and in costs of the system components can be realized.

The variable speed automotive air conditioning compressor, which can be characterized as having a substantial output capacity for its size and specified speed range and being vibration resistant, can be utilized for cooling and heating applications. Since the compressor capacity is a function of the speed, the variable speed compressor could be adapted to variable winds for energy conversion in the agricultural sector.

The primary objective of the project is to design an unguyed wind energy conversion system consisting of a Savonius rotor assisted non-articulating 5 m (15 ft) diameter Darrieus vertical axis wind turbine, which is self-starting, and is mechanically coupled by a V-belt drive to an automotive air conditioning variable speed compressor. The variable speed compressor is utilized as a mover for a variable speed heat pump system.

The basic objective is further subdivided into the following objectives:

1. To develop a preliminary design of the wind energy conversion system, which later can be modified to the existing energy needs.
2. To predict the performance of the wind energy thermal system through analysis and integration of the performance characteristics of the system components.

LITERATURE REVIEW

Power in the Wind

The variables that influence the power availability in the wind are density of the air, velocity of the air and the stream tube area, Johnson (32). The ideal available power or wind potential in the wind stream consists of two components. One component is the kinetic energy of the air and the other is the mass flow of the air. The product of these two terms is the power available in the stream tube:

$$P = (\tfrac{1}{2}V^2)(\rho AV) = \tfrac{1}{2}\rho V^3 A \qquad (1)$$

where P = available wind power, watts

ρ = air density, kg/m^3

A = stream tube cross-sectional area, m^2

and V = velocity of the wind, m/s.

Any turbine size can theoretically be located at any given turbine site. Therefore, the ideal available power can also be expressed as the power per unit area or power flux:

$$P/A = \tfrac{1}{2}\rho V^3, \text{ watts}/m^2 \qquad (2)$$

The air density of wind power is a function of pressure, temperature and relative humidity:

$$\rho = 1.2929 \frac{(P_r - VP)}{760} \frac{273}{T}, \text{ kg}/m^3 \qquad (3)$$

where P_r = pressure, mm of Hg

T = temperature, degrees Kelvin

and VP = vapor pressure of water vapor, mm of Hg

The vapor pressure can be found, if dew point is known, but since the vapor pressure affects the density by less than one percent it is

usually dropped from the calculation, Golding (25) and Johnson (32).

Wind turbine performance is generally characterized by a power conversion efficiency, or the ratio of wind turbine shaft power to the power passing through the stream tube:

$$C_p = \frac{P_s}{\frac{1}{2}\rho A V^3} \tag{4}$$

where C_p = turbine conversion efficiency referred to as coefficient of performance, dimensionless

P_s = turbine shaft power, watts

ρ = air density, kg/m^3

V = velocity of the wind, m/s

and A = turbine stream tube corss-sectional area, or turbine swept area, m^2 (area outlined by the intersection of the rotating blades and the plane which is perpendicular to the wind stream and intersects the turbine rotation axis)

$$P_s = T\omega \tag{5}$$

where P_s = turbine shaft power, watts

T = average total turbine blade torque, N·m

and ω = turbine rotor angular velocity, rad/s

When the power in the wind is converted to mechanical power with an efficiency C_p, which is transmitted to the generator through a mechanical transmission with efficiency n_m, and which is converted to electricity with an efficiency n_g, then the electrical power output is:

$$P_e = C_p n_m n_g P$$

Most wind turbines designed to produce power have some minimum wind speed, at which the system will overcome all mechanical and other

losses. This is called the cut-in speed, V_c. A wind speed at which a driven machine will produce its rated capacity is called the rated speed, V_R, and a design speed at which the wind machine is shut down to avert structural damage, is called the cut-out speed or furling speed, V_F.

For a given turbine, the rated speed can be increased by using a larger driven machine for a given wind turbine. This increases the static friction so that cut-in speed will increase, also. The cut-in speed is usually about one-half the rated wind speed, which corresponds to a cut-in power of one-eighth the rated power. The cut-out speed is usually three times the cut-in speed, Hagen (27). Also the cut-in wind speed should never be less than the average wind speed at the site, Park and Schwind (39).

Wind Statistics

Wind is a highly variable power source and there are several methods of characterizing this variability. One method is the power duration curve, which is an appropriate concept, but is not easily utilized for the selection of the cut-in wind speed, V_c, and the rated wind speed, V_R, for a given wind site, Johnson (32).

The most essential information, according to Golding (25) for evaluating the wind power potential at a given wind site, are the velocity duration curves or the velocity frequency curves and the power duration curves. The velocity duration curve is derived by analyzing the wind velocity data for a given time period and recording the information in a graphical form. The horizontal axis of the graph

usually depicts the number of hours in a year, the total being 8760, and the vertical axis is the wind velocity. Thus, the graph indicates the number of hours in a year during which the indicated wind velocity is exceeded. The velocity frequency curve is similar to the velocity duration curve, but the horizontal axis depicts the wind speed and the vertical axis illustrates the wind duration for a given time period.

A power duration or density curve is similar in form to the velocity duration curve and can be derived from the velocity duration curve since the power in the wind is proportional to the cube of the wind speed, as indicated in equations (2) or (6). The power duration graph indicates the number of hours in a year that the power output exceeds the indicated values. Figure 1 illustrates the annual power duration curve for Huron, South Dakota. The curve also indicates that the total amount of energy per year available in the wind per unit area is the area under the power density curve. Figure 2 compares the potential or the theoretical power density with the actual power density, which does not include the wind energy conversion system friction losses for a given wind turbine configuration. The actual power density is considerably less than the total available or theoretical power density. The actual power density depends on the cut-in wind speed, the rated wind speed, and the cut-out wind speed for the selected wind turbine, Cheremisinoff (17). Figure 2B illustrates the actual power density, which does not include the wind energy conversion friction losses, and is the shaded area under the graph, for a designated cut-in wind speed of 4.4 m/s (10 mph), rated wind speed of 14.5 m/s (33 mph), and a cut-out wind speed of 17.6 m/s (40 mph).

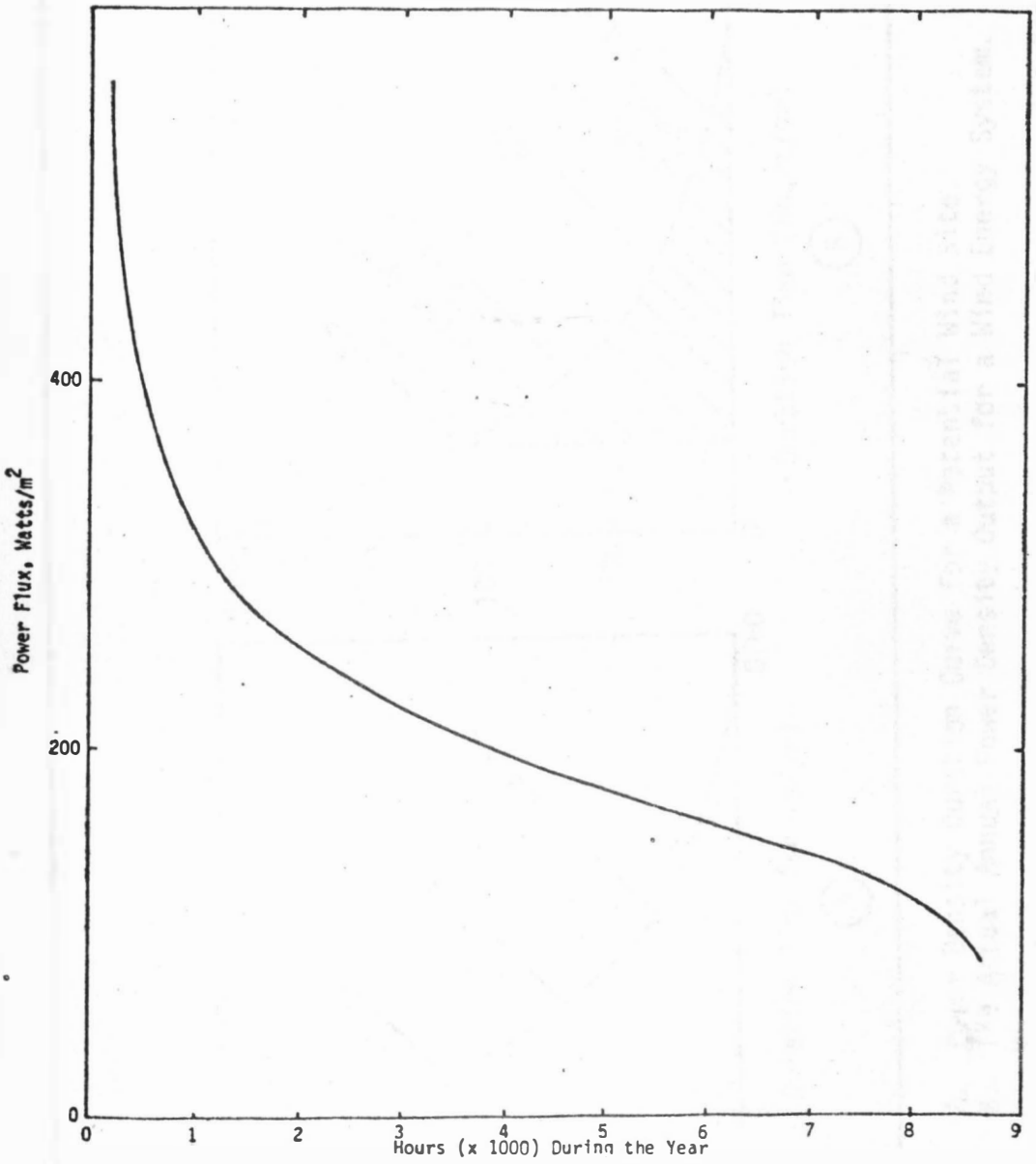

Figure 1. Power Duration Curve for Huron, South Dakota

From Verma (1979)

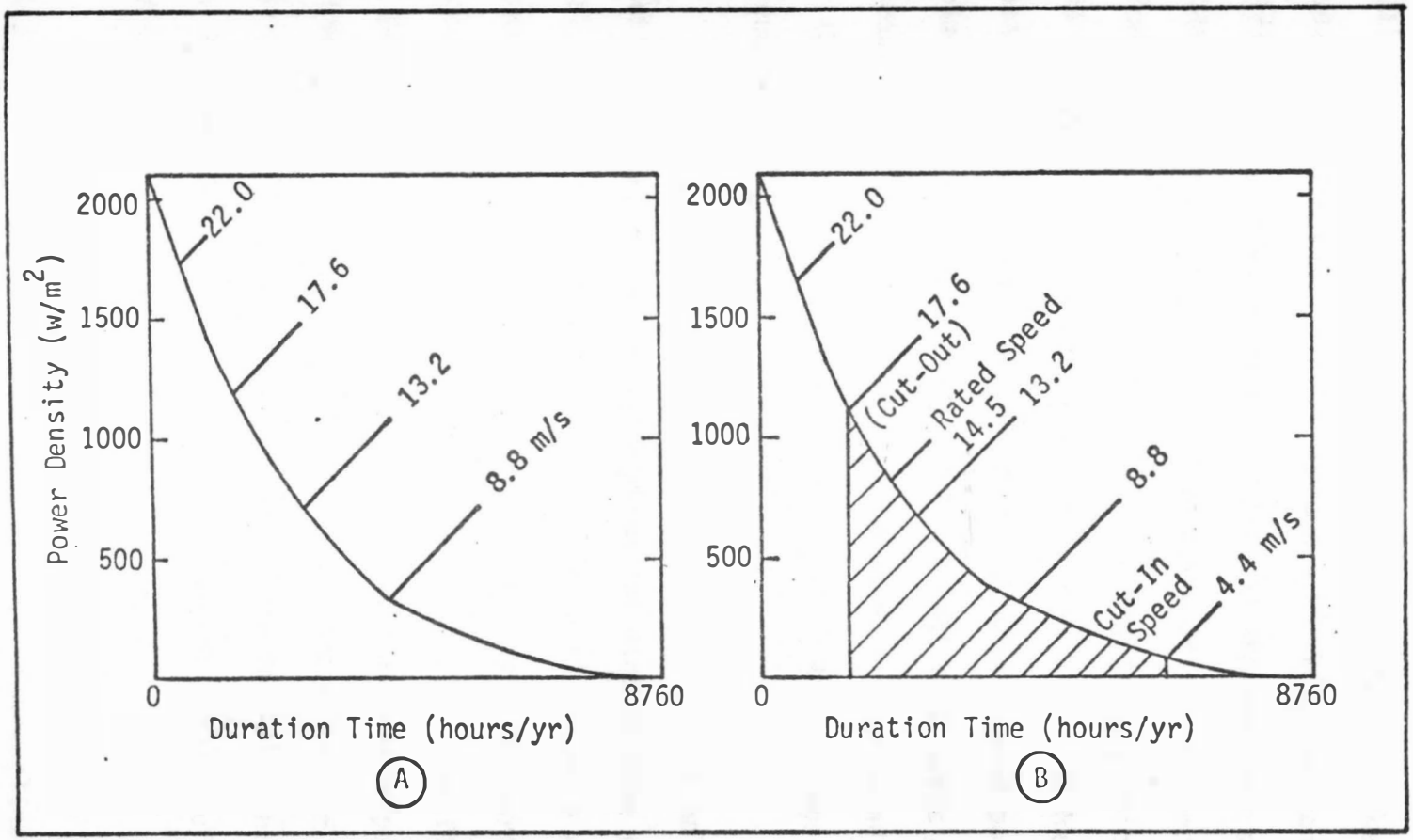

Figure 2. A. Power Density Duration Curve for a Potential Wind Site.
B. The Actual Annual Power Density Output for a Wind Energy System.

From Cheremisinoff (1978)

Wind gusts and relaxation periods or periods of calm are associated with the wind unpredictability. Therefore wind machines cannot be designed on the basis of the average wind velocity alone, Cheremisinoff (17). In addition, detailed statistical information, such as the standard deviations of the wind velocity or power associated with the wind must be carefully weighed against any designs which are based on the mean or average wind speeds, Hennessey (28). It has been estimated that, because of the cubic relationship between wind power and wind velocity, in conjunction with the fact that wind gusts and is seldom steady, the actual wind power available at a given wind site can be two or three times that derived on the basis of the average annual wind speeds, Eldridge (22).

Preliminary wind studies indicate that there is an optimum height that must be taken into consideration for wind machine design, Justus (33). The shape of the wind profile, as a function of height, is dependent upon the geographic, topographic, and the surface roughness factors, and upon the atmospheric stability of a specific wind site. In general, wind speed increases with the one-seventh power of the height, Johnson (32), Cheremisinoff (17), therefore the wind power increases to the three-seventh power of the height. This approximation has been observed to be valid for wind speeds capable of supporting moderate size wind generators, Cheremisinoff (17).

Another method, of characterizing wind variability, is the Weibull distribution or density function, which has been applied to the wind velocity data, Justus et al. (34), Johnson (32), Hennessey (28), Zimmer et al. (57). The method consists of evaluating the Weibull

distribution function parameters for given wind velocity data, which are utilized for computing the wind power, Johnson (32).

The Weibull distribution for a wind speed, V, is expressed by the probability density function, f(V), on the wind speed frequency curve.

$$f(V) = \left(\frac{k}{c}\right)\left(\frac{V}{c}\right)^{k-1} \exp\left[-\left(\frac{V}{c}\right)^{k}\right] \tag{7}$$

where c is the scale factor (units of speed) and, k the shape factor (dimensionless). The corresponding equivalent cumulative probability function, F(V), is

$$F(V) = 1 - \exp\left[-\left(\frac{V}{c}\right)^{k}\right] \tag{8}$$

Justus et al. (34) cite several advantages associated with the Weibull distribution function for processing wind data:

1. The Weibull distribution is a two-parameter distribution depending only on c and k, and is more general than the Rayleigh distribution (Rayleigh distribution is equation (7) with k=2).
2. The Weibull distribution has a computational advantage when compared to the more general bi-variable normal distribution, which requires five parameters.
3. The Weibull distribution displays reasonable fits to the observed wind distributions.
4. The Weibull parameters c and k at one known measured wind height can be utilized and adjusted to other desired wind heights.

By utilizing the Weibull distribution, Johnson (32) concludes that the shape parameter, k, is in the range $1.3 \leq k \leq 3$ for most wind regimes and the scale factor, c, is in the range $1.11\overline{V} \leq c \leq 1.13\overline{V}$.

Thus the scale factor, c, is directly proportional to the mean wind speed and is approximately 12 percent larger.

The Weibull distribution parameters c and k can be determined by the least squates approximation and from this data the total power in the wind for a specified wind speed interval can be determined, Reed (42). The decimal fraction of time, Δt between wind speed V_1 and V_2 is

$$\Delta t = \exp\left[-\left(\frac{V_1}{c}\right)^k\right] - \exp\left[-\left(\frac{V_2}{c}\right)^k\right] \tag{9}$$

Therefore, the total power in the wind, P for a unit wind speed interval is

$$P = CA \sum_{i=1}^{n} (\Delta t_i)(\overline{V}_i)^3 \tag{10}$$

where n = number of total intervals

$\overline{V}_i$ = the mean wind speed in the interval

A = area

Δt_i = time interval

C = coefficient dependent on the selected units

Jayadev (31) also concludes that the annual production of the generated power can be determined by multiplying the ideal available wind power or equation (1) by the applicable efficiencies (C_p, n_m, n_g) of the wind generating system at each prevailing wind speed and then integrating over a one-year interval.

The power determined using average wind speed methods will not optimize the selection of the rated wind speed, V_R, and the cut-in wind speed, V_c, and is not very useful for the wind turbine economic studies, Johnson (32). A more refined method can be realized by utilizing the

wind energy factor, WF and selecting the rated wind speed, V_R (or V_R/c), for maximizing the wind energy factor, WF. This permits the wind system to produce the maximal possible energy per unit area of the rotor.

The wind energy factor, WF is defined as

$$WF = \frac{(S_1 + S_2)}{c^3} \tag{11}$$

where $$S_1 = kc^3 \int_{V_c/c}^{V_R/c} \left(\frac{V}{c}\right)^{k+2} \exp\left[-\left(\frac{V}{c}\right)^k\right] d\left(\frac{V}{c}\right) \tag{12}$$

and $$S_2 = V_R^3 \exp\left[-\left(\frac{V_R}{c}\right)^k\right] = c^3 \left(\frac{V_R}{c}\right)^3 \exp\left[-\left(\frac{V_R}{c}\right)^k\right] \tag{13}$$

Figure 3 depicts the plot of the wind energy factor, WF versus V_R/c for various values of k for $V_c = 0.5V_R$. For example, if a wind site is selected where k = 2.4, the energy produced per unit area can be maximized if $V_R/c = 1.7$ or $V_R = 1.7c$. Since $c = 1.12\overline{V}$, the rated speed is about 1.9 times the mean wind speed. For comparison, Johnson (32) has plotted the Weibull power density, w/m^2 as a function of the rated wind speed, V_R for identical wind data, Figure 4. The curve designated "Weibull" was computed from the c and k parameters and the curve designated "calculated" was computed by utilizing the actual power equation (6).

Figure 5 illustrates the two parameter Weibull wind density function and the cumulative Weibull density function for Huron, South Dakota. Based on published Weibull distribution parameters and available wind data for Huron, South Dakota, from 1965 to 1976, Verma (55) has

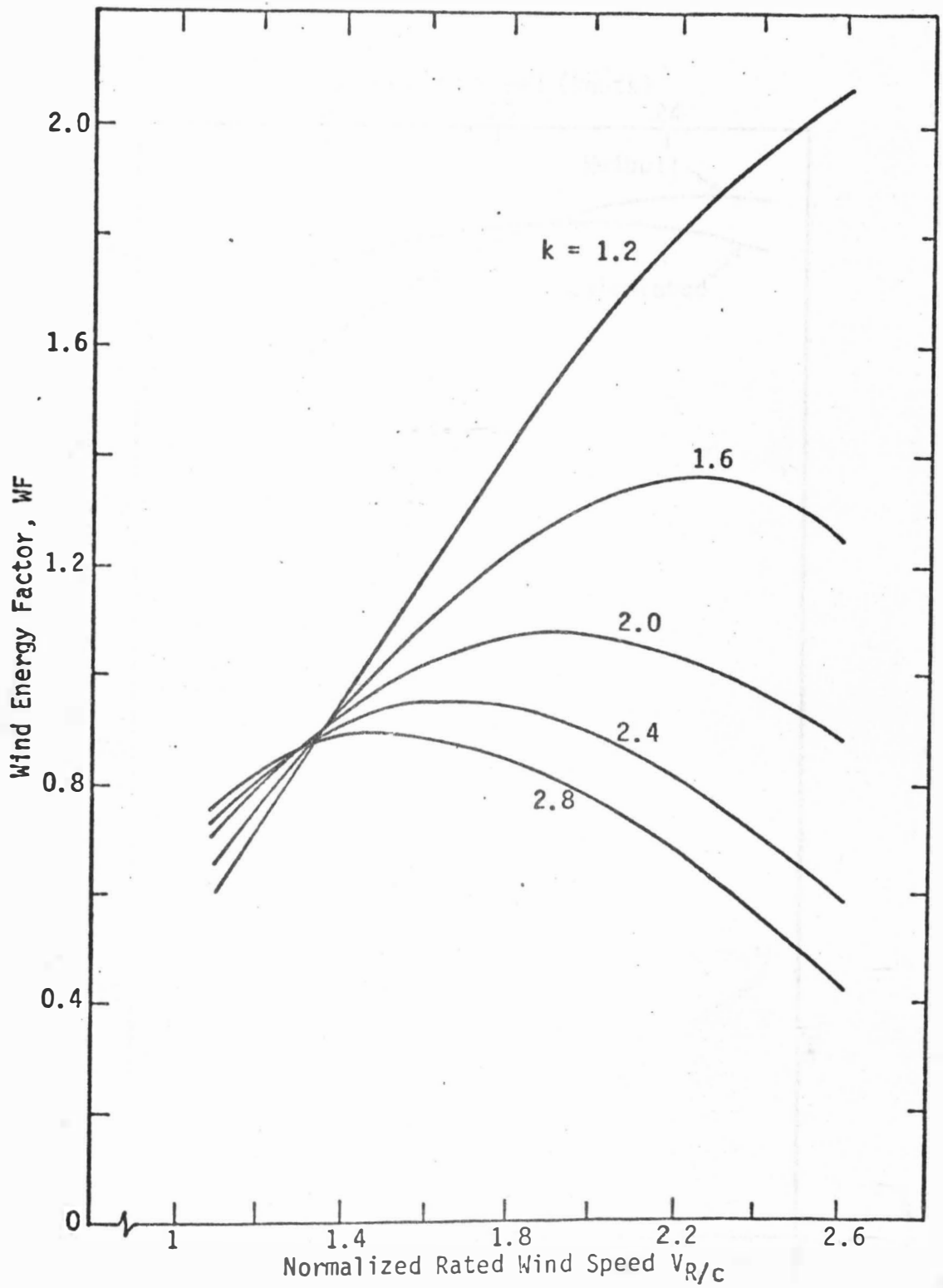

Figure 3. Wind Energy Factor for a Cut-In Speed of ½ the Rated Speed

From Johnson (1978)

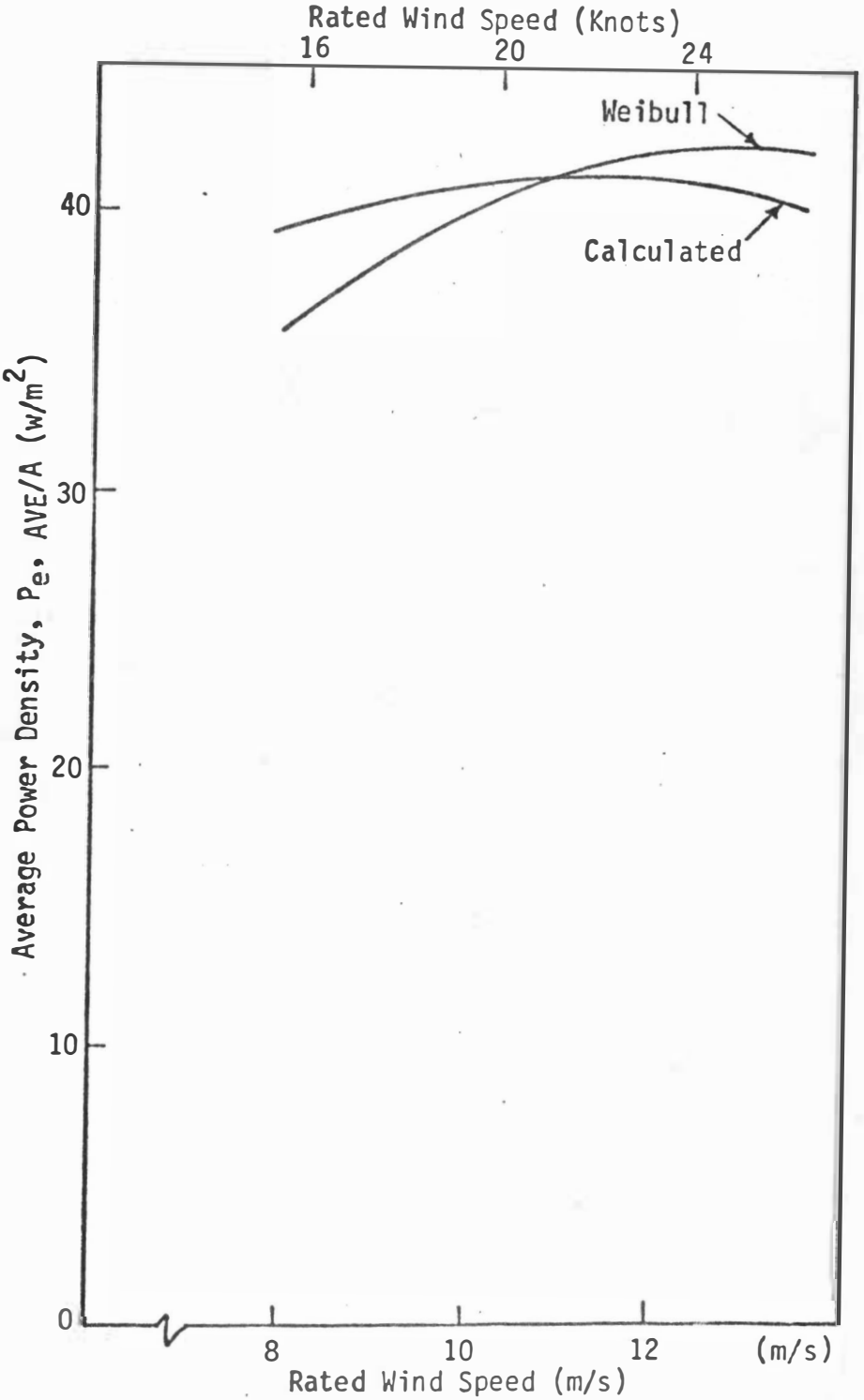

Figure 4. Average Power Density at Russell, Kansas 1950-67, 1970-73. Anemometer Height is 29 feet.
From Johnson (1978)

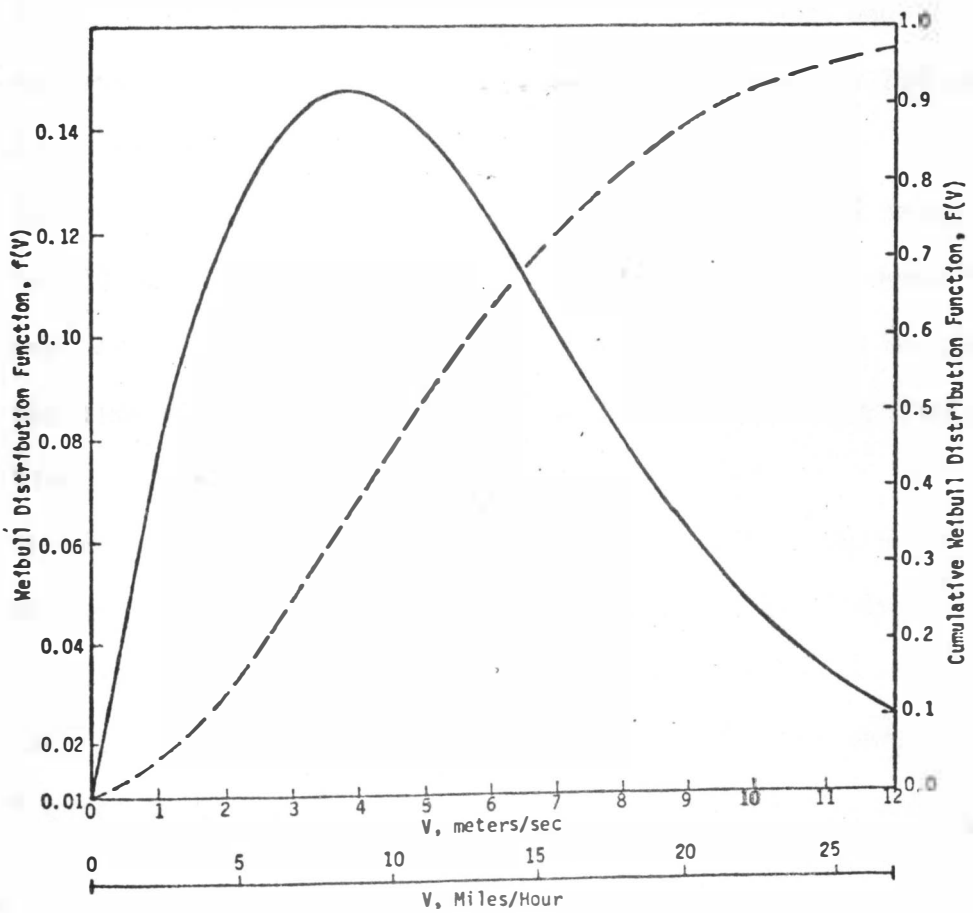

Figure 5. Annual Average Wind Speed Distribution Function for Huron South Dakota.

From Verma (1979)

calculated the available wind power flux for the area. Also the combined potential of wind and solar energies was evaluated for the area. The conclusions from this study are:

1. The average annual wind speed for the area is 5.1 m/s (11.5 mph). April has the highest average wind speed of 5.9 m/s (13.3 mph) and July has the lowest average wind speed of 4.5 m/s (10.3 mph).
2. Wind power intensity reaches a peak at about 1600 hours during a day and the average wind intensity is approximately 210 watts/m^2 (19.5 watts/ft^2), Figure 6.
3. The power duration curve, Figure 1, shows that wind power levels up to 100 watts/m^2 (9.3 watts/ft^2) can be expected for over 95 percent of the time, 200 watts/m^2 (18.6 watts/ft^2) for 50 percent of the time and 300 watts/m^2 (27.9 watts/ft^2) for 13 percent of the time.
4. Combining wind and solar energies significantly improves the energy density flux of these alternate energies for East Central South Dakota, Figure 7. The two energies compliment each other well to make the total energy more uniform than either of them alone, Figures 8, 9 and 10.

Wind Energy Conversion Systems

The utilization of alternate energy sources, in agricultural production systems, continues to receive attention due to the shortages and rising costs of fossil fuels. Several viable options to direct utilization of fossil fuels are possible. Wind and solar energies offer at least two possible alternate energy sources, which can be

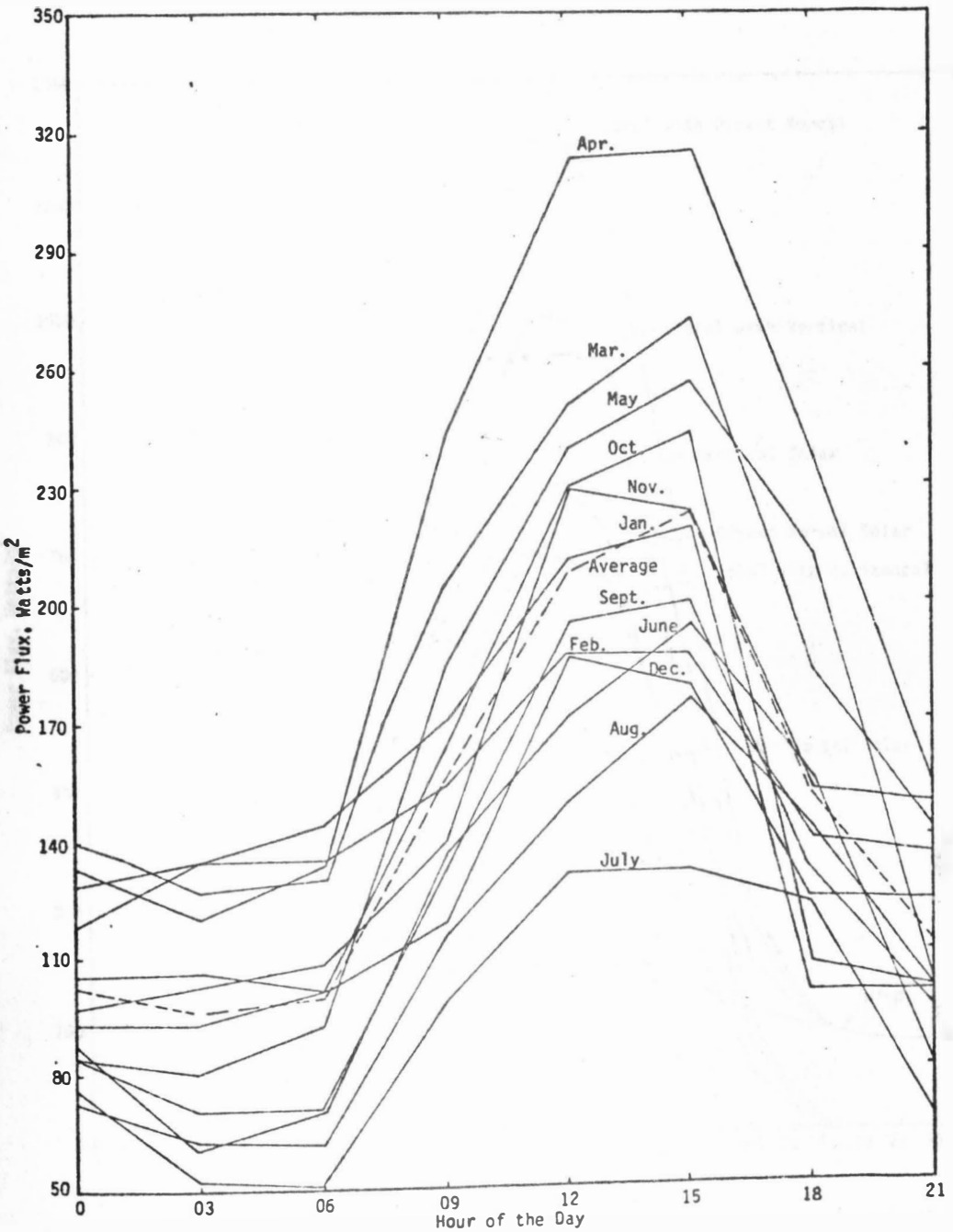

Figure 6. Diurnal Variation in Wind Power for Different Months at Huron, South Dakota From Verma (1979)

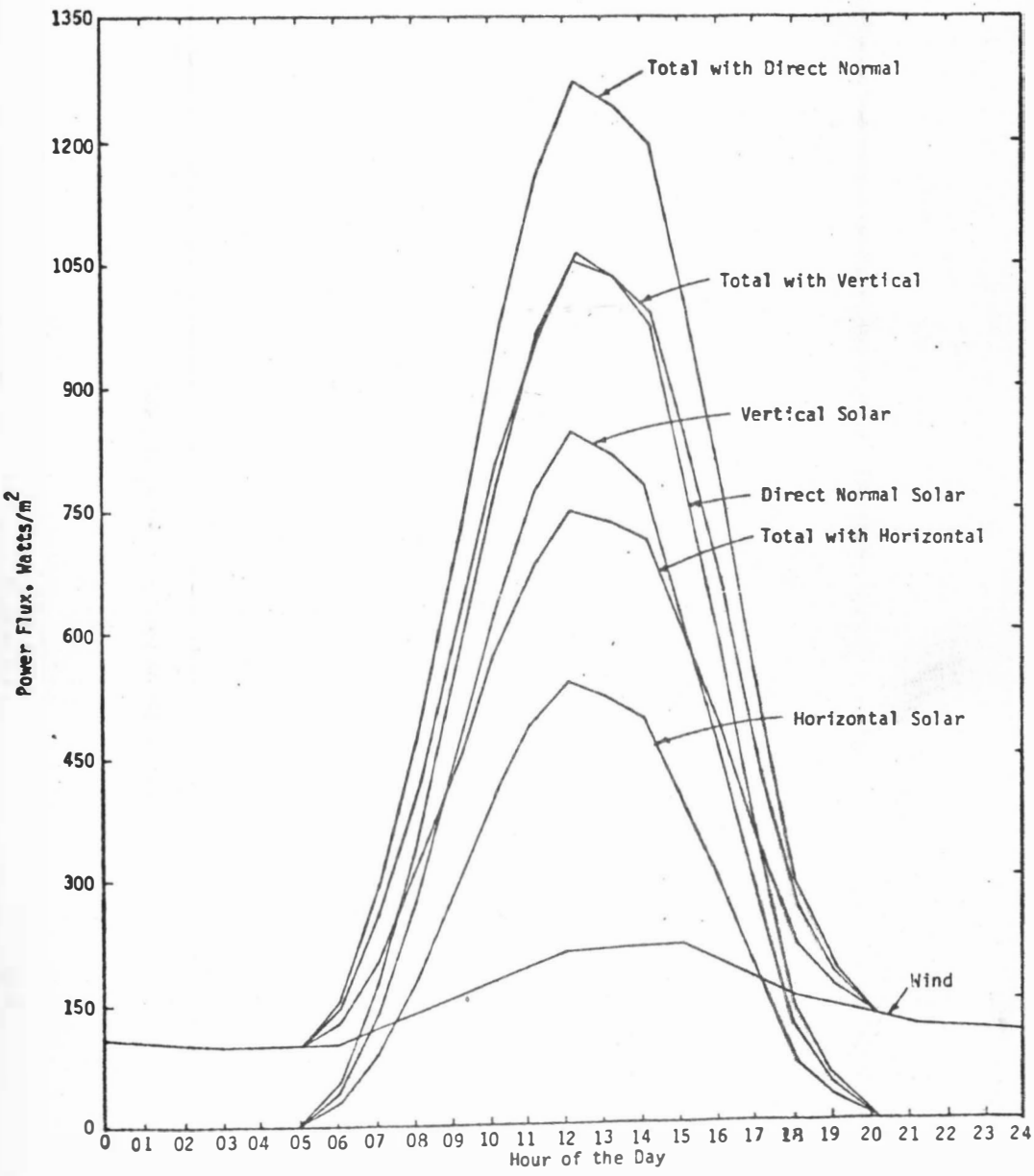

Figure 7. Average Diurnal Variation in Wind and Solar Energy Intensities for Huron South Dakota

From Verma (1979)

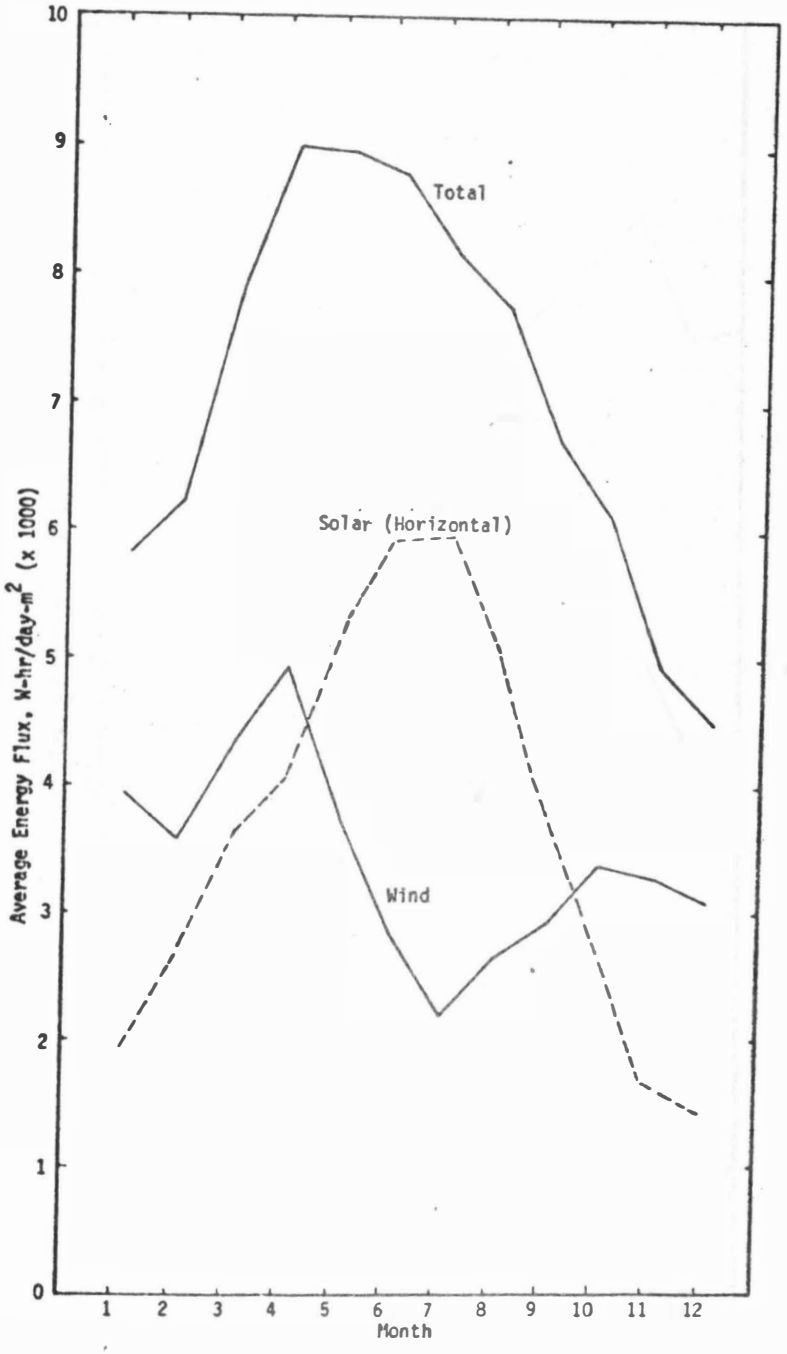

Figure 8. Yearly Variation in Wind and Solar (Horizontal) Energies for Huron, South Dakota.

From Verma (1979)

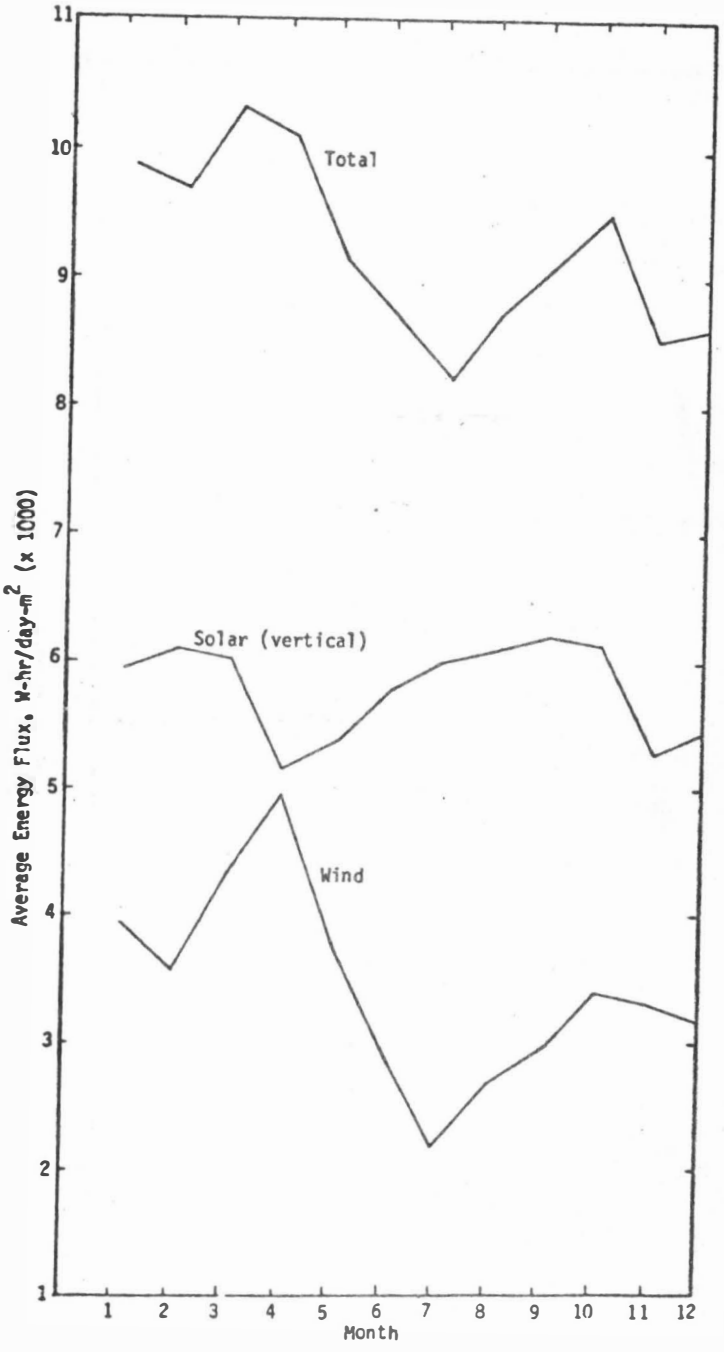

Figure 9. Wind, Solar (Vertical), Wind and Solar (Vertical) Total Energies for Huron, South Dakota.

From Verma (1979)

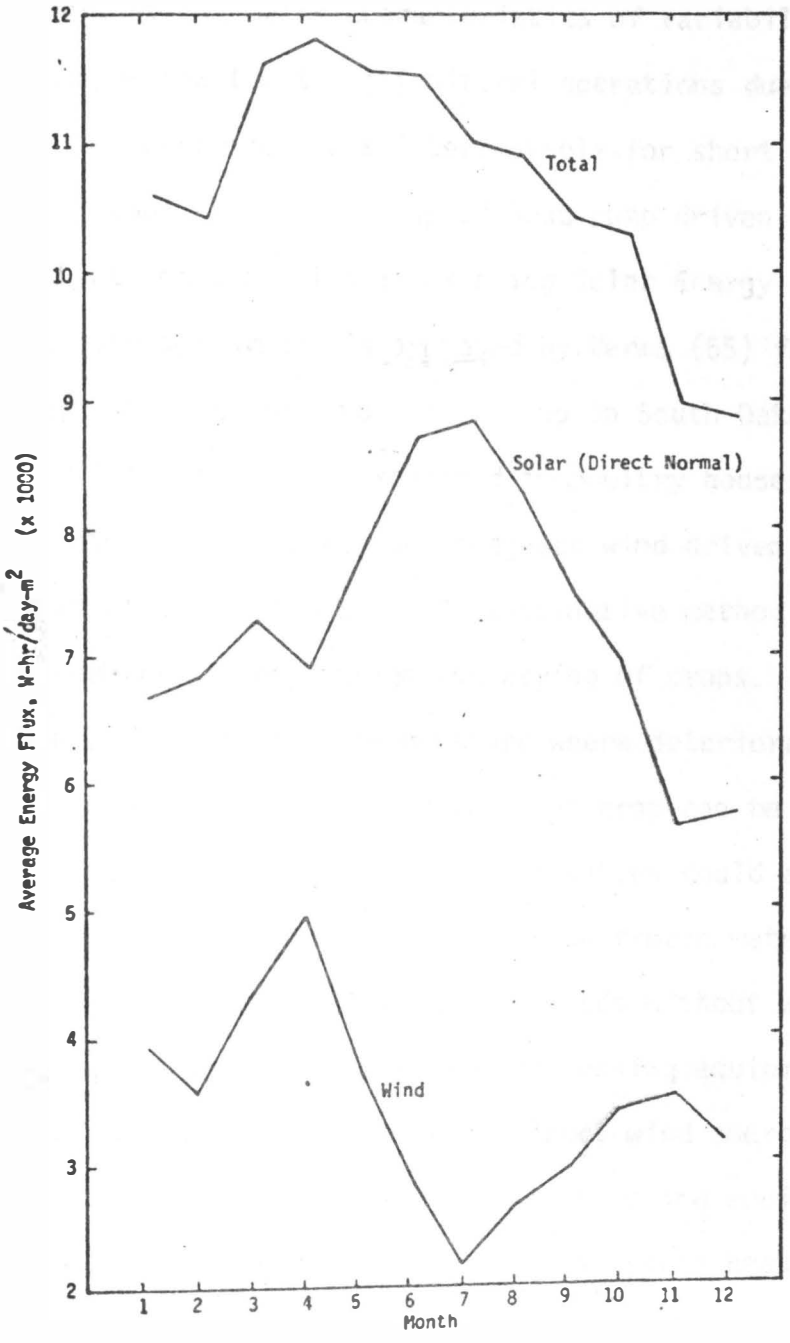

Figure 10 Wind, Solar (Direct Normal), and Total Energies for Huron, South Dakota.

From Verma (1979)

utilized as supplemental energy sources in conjunction with conventional energies.

Wind power, having major characteristics of variability and discontinuity, can be adapted to agricultural operations due to the fact, that several farm operations are interruptable for short periods of time, Liljedahl (36). A variable speed heat pump driven by a vertical axis wind turbine together with an existing Solar Energy Intensifier-Thermal Energy Storage System is proposed by Verma (55) for on-farm space heating, water heating and crop drying in South Dakota. Further, fossil fuel savings can also be realized in poultry houses and swine finishing buildings. Liljedahl (36) suggests wind driven fans to dry crops or grains with unheated air. An alternative method is to use wind power for refrigerated storage and drying of crops. This application cools the moist crop to a temperature where deterioration is reduced for long periods of time and then the crop can be dried at a slower rate. Dairy products and stored vegetables could also be refrigerated with wind driven machinery, using frozen water or solutions to store cooling capacity to accommodate periods without wind. Wind energy can also be used for driving feed processing equipment. Gunkel and Furry (26) described an operational, direct wind energy, heated, water system for washing and sanitizing milk handling equipment. In addition, the hot water produced can be used as space heating for rural residences. Also an operational, combined wind turbine, electric generator, and heat pump system is being utilized to cool milk and heat water on a dairy farm, Cummings (21). Galanis and Delisle (23) propose a wind turbine driven heat pump that will absorb heat from the

ground for heating a rural residence. While a wind driven aeration system for waste waters is proposed by Galanis, Narasiah and Dang (24). A wind energy conversion system consisting of a wind generator, heat pump, water heater and energy storage has been successfully used for electric load leveling on rural power systems, and for rural heating loads, Soderholm (47). Cromack and Heronemus (20) propose a combined wind, solar, and thermal storage system for residential heating.

Hughes and Dunn (30) described an existing wind turbine, electric generator, energy conversion system for feeding "excess" power directly into the power line with no intermediate storage. A wind driven electric generator capable of specific output within 80 percent of the maximum for a wide range of wind speeds has been proposed by Johnson (32). Biederman (9) proposes a 5- to 10-Kilowatt, wind powered hydrogen/electric system for use in rural and farm settings, with the mechanical shaft horsepower from the turbine converted to electricity and the produced hydrogen used for fuel and a storage medium.

Clark and Schneider (19) describe a wind assisted electric irrigation pumping system for large scale irrigation. A small Savonius rotor-diaphragm pump irrigation system has been successfully demonstrated by Simonds and Bodek (46).

Darrieus Vertical Axis Wind Turbine

Wind was probably one of the first energy sources to be harnessed by man, Blackwell et al. (15). History indicates that windmills were used in Babylon and China around 1700 to 2000 B.C., in Persia around 644 A.D., and in Europe starting from the eighth century on, Golding (25),

and over the past centuries several million windmills have been used in such applications as grinding grain, pumping water, and generating electricity. Several decades ago, the most widely accepted wind machines in the United States were the fixed pitch horizontal axis wind machines such as the "American Windmill" and the propellor type, which were utilized to pump water and generate electricity in rural areas, Blackwell and Feltz (11).

One of the most promising of the fixed-pitch vertical axis wind turbines is the Darrieus rotor. Although a patent was issued in 1933 to George Darrieus by the United States Patent Office, it appears that the concept lay dormant until the mid 1960's, when South and Rangi (49) of the National Research Council of Canada independently developed the concept, Blackwell et al. (15).

Darrieus Vertical Axis Wind Turbine Performance Characteristics

The Darrieus vertical axis wind turbine is basically a lift-driven machine, with blades of symmetric airfoil cross section, bowed outward at the midpoint and attached at both ends to a rotational axis perpendicular to the airstream. If the blades are formed in this shape, rotation will not cause the blades to deform as a result of bending loads and thus the stresses will be in pure tension, Blackwell and Feltz (11).

The wind velocity acting on a blade section consists of two components: one component due to the velocity of the blade as it rotates and the other due to the wind velocity. The velocity components form a resultant velocity vector that acts at a particular angle (angle of

attack, α) relative to the airfoil chord line (a straight line joining the trailing and leading edges of an airfoil) producing lift and drag forces. Resolving the lift and drag forces along the blade chord line will determine the force which produces a torque in the direction of blade rotation, and from this torque turbine shaft power can be developed.

Large angles of attack common to low rotational speeds will cause the Darrieus wind turbine to stall, and theoretically the turbine will not be self-starting, Blackwell and Feltz (11). Although a two-bladed Darrieus wind turbine has been known to be self-starting, Chasteau (16), Clark (18) also reports that three-bladed Darrieus turbines are known to be self-starting.

Because the blades stall at low relative rotational speeds an auxiliary starting device is needed for the Darrieus wind turbine. A Savonius rotor with drag buckets attached to the central shaft has been utilized as a starter, Blackwell (11). Kulgren, Wiedemier and Tinsley (35) have demonstrated that where a single, three-bladed Savonius rotor is sized so that its length is equal to the Darrieus equatorial diameter, the Savonius positive torque range will be extended at higher Darrieus tip speed ratios. The Savonius rotors are located at the top and bottom on the vertical shaft to minimize airflow interference with the Darrieus blades. Weingarten and Blackwell (56) state that the center 56 percent of the vertical height produces over 90 percent of the theoretical maximum energy that would be developed if the entire blade length were a true airfoil. In addition, the Savonius rotor has good torque characteristics at low rotational speeds, and is sized so that when the blades are

operating at the most efficient condition, the starter is also operating at the most efficient condition, Blackwell and Feltz (11), Banas and Sullivan (7).

Darrieus wind turbines are also competitive with high-performance propeller-type wind turbines and Blackwell et al. (15) have listed the following advantages:

1. Vertical turbine symmetry accepts wind from any direction thus eliminating need for yaw control mechanisms.
2. The vertical turbine shaft allows power conversion equipment to be placed near ground level. Such placement will decrease tower requirements, dimensions and weight constraints on the gearbox and other mechanical components, and facilitates equipment maintenance.
3. Attachment of blades at two points, as well as troposkein (Greek meaning turning rope) curved-blade shape, reduce airfoil structural requirements.
4. Lower rotor speed increases gearbox torque rating for a given power rating.

Wind turbine efficiency or coefficient of performance, C_p is not a constant for the rotor, rather is depends on several parameters, including turbine configuration, size, rotational speed, wind speed, and flow properties of the air through the turbine. A convenient means of characterizing the aerodynamic performance of any wind turbine may be achieved by plotting power coefficient, C_p versus tip speed ratio, Figure 11.

Tip speed ratio is defined as:

$$X = \frac{R\omega}{V} \tag{14}$$

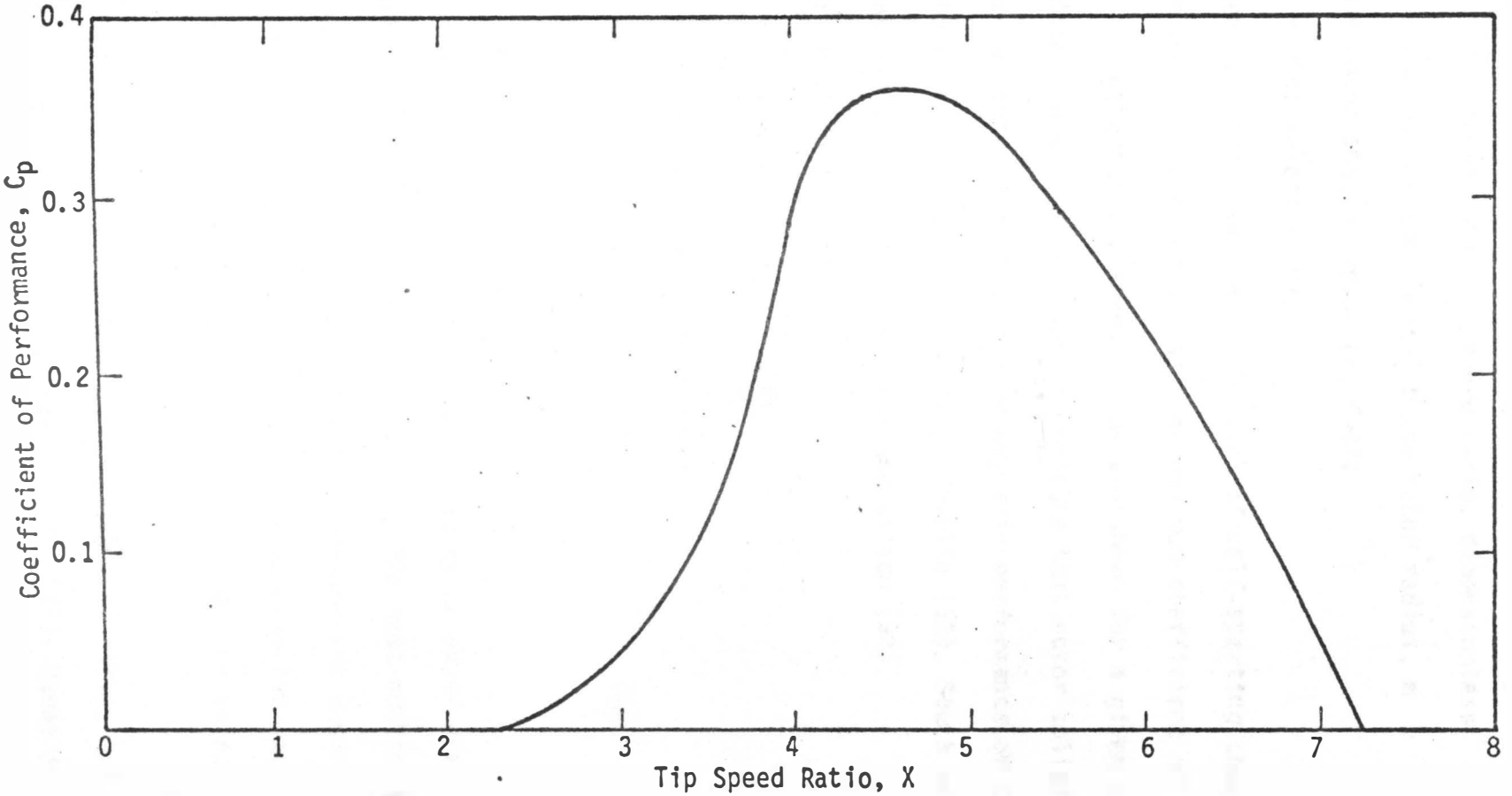

Figure 11. Power Coefficient Versus Tip Speed Ratio for a Three Bladed Darrieus Vertical Axis Wind Turbine.

From Banas et al. (1975)

where X = tip speed ratio, or speed ratio, dimensionless

R = maximum or equatorical blade rotor radius, m

ω = rotor angular velocity, rad/s

and V = wind velocity, m/s

Figure 11 clearly indicates the lack of self-starting characteristic of the Darrieus turbine. Also, the maximum coefficient of performance and the expected tip speed ratios are shown for a given turbine configuration. Wind turbine studies indicate that rotor solidity, σ, is another parameter affecting the aerodynamic performance of the Darrieus turbine, Blackwell et al. (15), Templin (52), South and Rangi (49), Banas and Sullivan (7), Thresher and Wilson (54).

Rotor solidity is defined as:

$$\sigma = \frac{Nc}{R} \tag{15}$$

where σ = rotor solidity, dimensionless

N = number of turbine blades

c = airfoil chord length, m

and R = rotor maximum radius, m

Figure 12 presents the effects of rotor solidity on power coefficient for a constant Reynolds number of 0.3×10^6. The most noticeable influence of solidity is that as solidity decreases the entire C_p curve is shifted to higher speed ratios. To maximize the power coefficient, a solidity in the range of 0.2 to 0.25 should be selected, Blackwell, Sheldahl and Feltz (14).

Darrieus wind turbine rotor height to diameter ratio, λ, also affects the performance curve, Blackwell et al. (15), Banas and

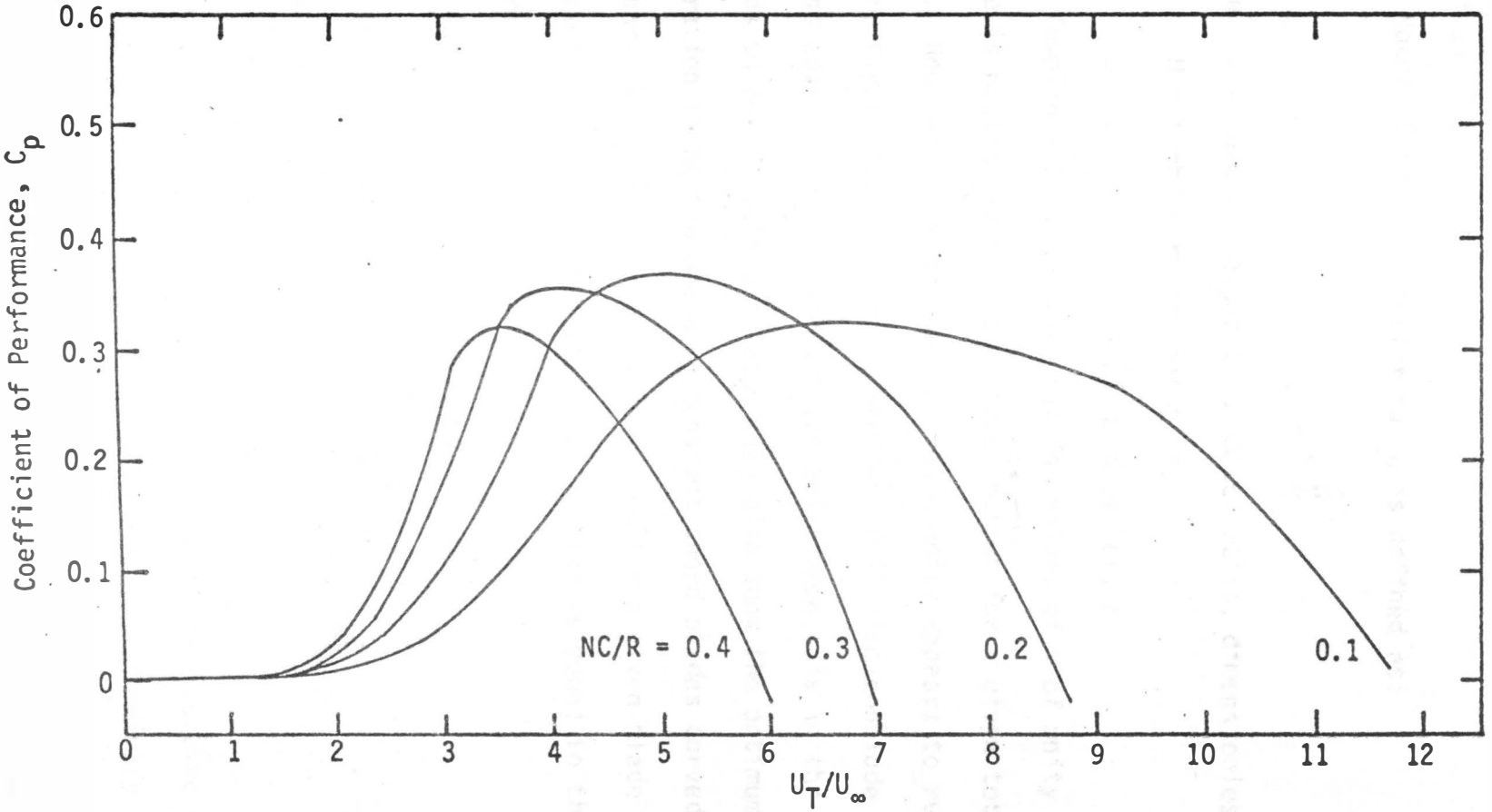

Figure 12. The Effect of Solidity on Coefficient of Performance, C_p ($R_e = 0.3 \times 10^6$) for a Darrieus Wind Turbine.

From Strickland (1975)

Sullivan (7).

Rotor height to diameter ratio is defined as:

$$\lambda = \frac{H}{D} \tag{16}$$

where λ = turbine height to diameter ratio, dimensionless

H = turbine rotor height, m

and D = turbine rotor maximum diameter, m

Templin (52) indicates that for values of λ of unity and greater, there is negligible effect on power output for a given total swept area. However, a reduction of λ below unity appears to reduce maximum power, Figure 13. Reuter and Sheldahl (44) also conclude that no significant advantages or disadvantages exist when λ is in the range of two-thirds to one. South and Rangi (48) also show the optimum rotor configuration to be the one with constant chord blades curved into a catenary that encloses the maximum area for a given blade length, and the swept area is maximum when the diameter is equal to the height of the rotor.

Turbine swept area is defined as:

$$A = \frac{2}{3}D^2 \tag{17}$$

where A = turbine swept area, m^2

and D = turbine maximum diameter, m

Since the Darrieus turbine is a lift device, turbine performance is a function of the Reynolds number, and, if the primary torque producing portion of the blade near the equatorial plane is operating at high tip-speed ratios, it appears that the most appropriate velocity

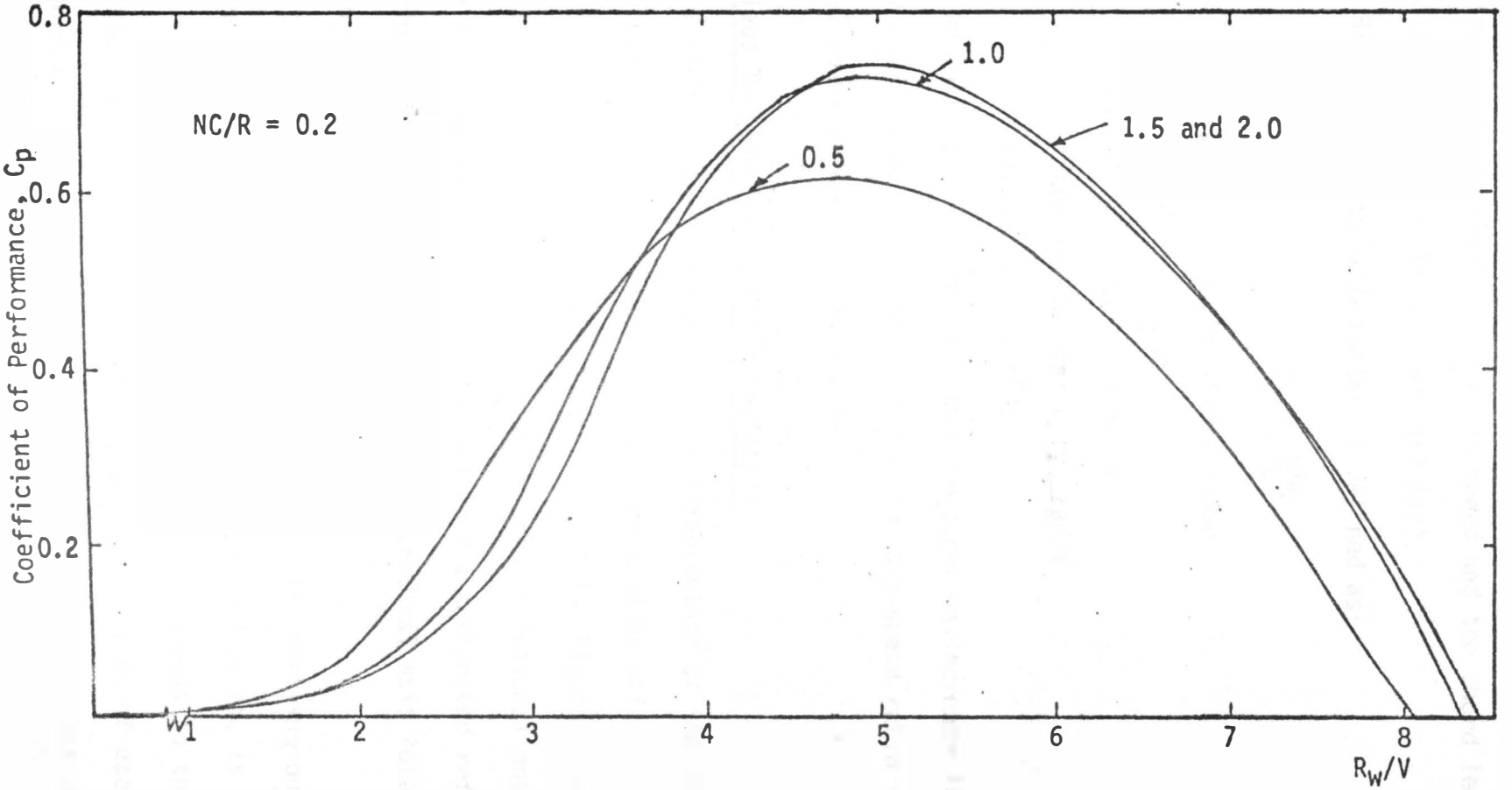

Figure 13. Coefficient of Performance, C_p vs Height to Diameter Ratio, λ for a Three Bladed Darrieus Vertical Axis Wind Turbine

From Templin (1974)

and length scales are the blade tip speed and the chord length, respectively, Blackwell and Sheldahl (12).

Blade chord Reynolds number is defined as:

$$R_{ec} = \frac{cR\omega}{\nu} \tag{18}$$

where R_{ec} = blade chord Reynolds number

c = chord length, m

R = rotor maximum radius, m

ω = rotor angular velocity, rad/s

and ν = air viscosity, m^2/s

An increase in Reynolds number produces an increase in the maximum power coefficient, and also increases the tip-speed ratio range for useful power production, Figure 14.

Darrieus Turbine Torque Characteristics

Variable torque is considered a disadvantage of the vertical axis wind turbine, but this effect can be minimized by utilizing a three-bladed rotor design, Blackwell and Feltz (11). Figure 15 presents actual torque to maximum torque ratio versus rotational angle, Θ (overall angle of rotation of a blade measured from a designated reference point) for single, two-bladed, and three-bladed vertical axis rotors transversing one complete revolution.

The torque developed by a single blade transversing one complete revolution and operating at an optimum tip speed ratio, is constantly changing, being maximum where the blades are sideways to the wind on both the upwind side as well as on the downwind side of each revolution. The torque becomes slightly negative in the two positions where the

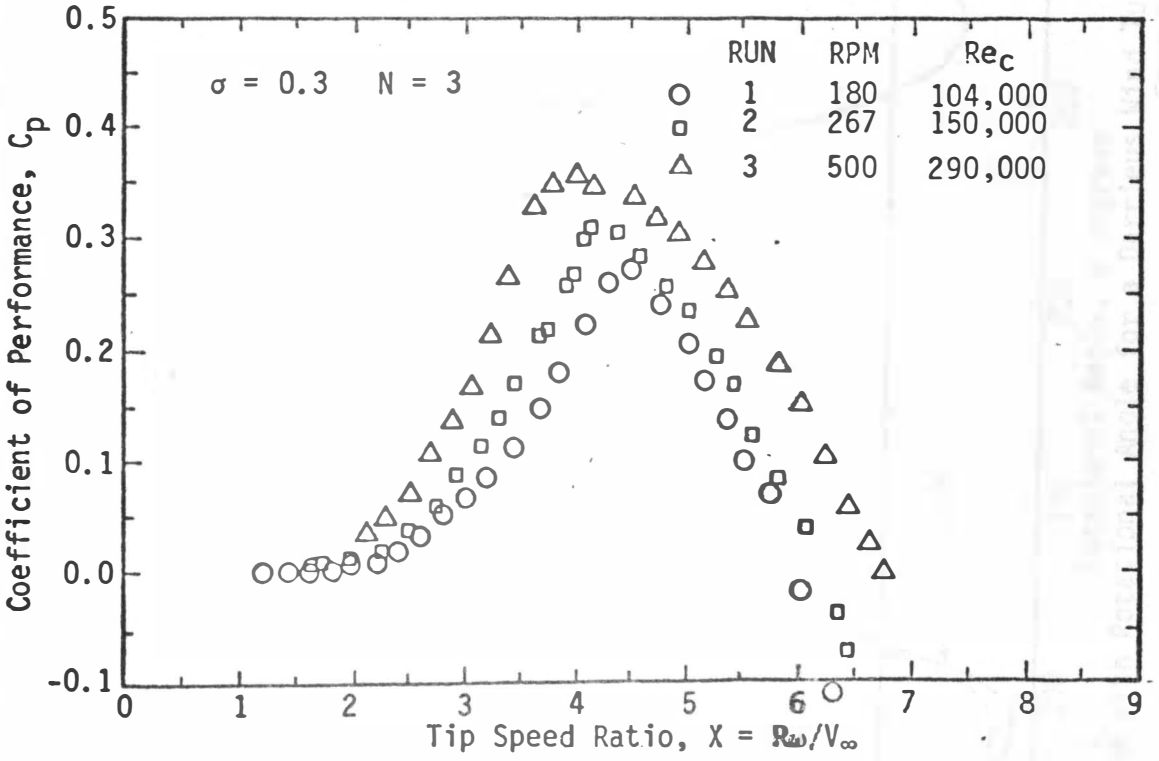

Figure 14. Influence of Reynolds Number on Power Coefficient for Solidity of 0.3 for a Three-Bladed Darrieus Vertical Axis Wind Turbine.

From Blackwell and Sheldahl (1976)

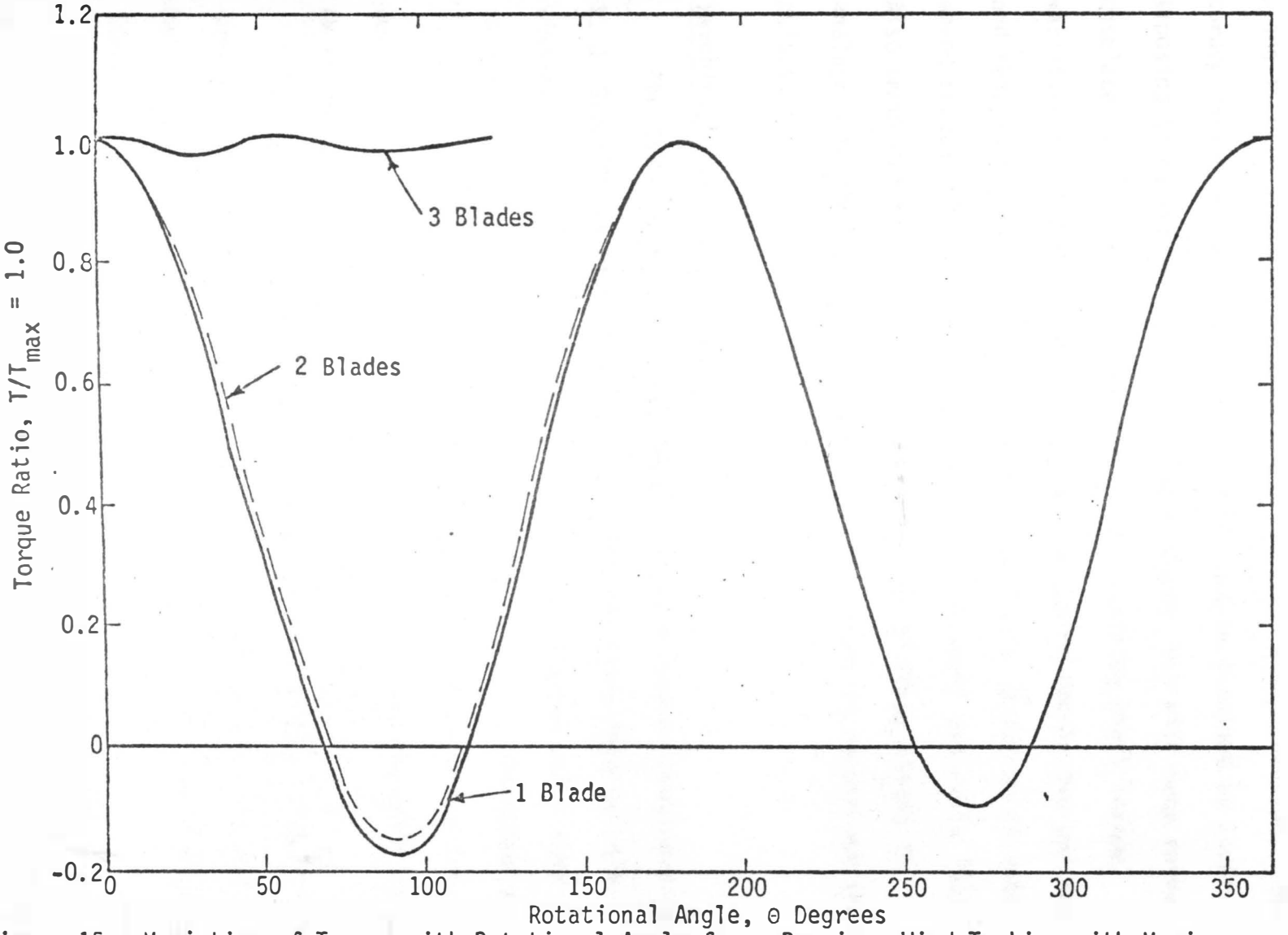

Figure 15. Variation of Torque with Rotational Angle for a Darrieus Wind Turbine with Various Numbers of Blades. From Blackwell and Feltz (1975)

blade is driving directly into or away from the wind direction. The torque variation for a three-bladed rotor can be obtained by superimposing three torque curves for single blades, but with each curve displaced 120^{o} from the other blade. The resulting shaft torque variation for a three-bladed rotor will be approximately two percent, and this torque variation will cause a negligible variation in rotor speed because of the inertia of the rotor, Blackwell and Feltz (11). Also smoothing of the torque curve by the use of three blades is analogous to the three phasing of electrical power to smooth out the pulsations.

Savonius Rotor

The Savonius rotor is a vertical axis wind turbine developed by S. J. Savonius, a Finnish engineer, during the years 1925 to 1928, Simonds and Bodek (46). Applications for the Savonius rotor have included pumping water, driving an electric generator, providing ventilation, and providing water agitation to keep stock ponds ice free during the winter. A common application for the Savonius rotor is as an ocean current meter, Blackwell, Sheldahl and Feltz (13).

The construction of a Savonius rotor is very simple. The rotor consists of two buckets or a cylinder cut lengthwise with the two halves held at the ends by two end plates and rotating about a vertical axis, Simonds and Bodek (46).

The Savonius rotor has very good starting torque characteristics and favorable torque capabilities at low rotational speeds as compared to the Darrieus rotor. Due to these favorable torque characteristics,

the Savonius rotor can be utilized as a passive starter for the Darrieus wind turbine, Blackwell (10).

Important parameters affecting the performance of a Savonius rotor are: the coefficient of performance C_p, torque coefficient C_T, tip speed ratio X, and the gap dimension or gap width s/d. The power coefficient, C_p for a Savonius wind turbine is defined as:

$$C_p = \frac{T\omega}{\frac{1}{2}\rho V^2 R A_s} \tag{19}$$

where T = shaft torque, n-m

ω = shaft rotational speed, rad/s

ρ = free stream air density, kg/m^3

V = free stream velocity, m/s

A_s = projected swept area of the rotor, m^2

The power coefficient is the ratio of the turbine power output to the total power in the air stream tube, A_s, Banas and Sullivan (8), Blackwell, Sheldahl and Feltz (13), Simonds and Bodek (46). Another important parameter for the Savonius rotor is the torque coefficient, C_T defined as:

$$C_T = \frac{T}{\frac{1}{2}\rho V^2 R A_s} \tag{20}$$

The tip speed ratio or speed ratio, X is defined as:

$$X = \frac{R\omega}{V} \tag{21}$$

where the values are defined as before.

Figure 16 depicts a typical performance curve of a Savonius rotor as compared to a Darrieus wind turbine. The gap width or gap dimension

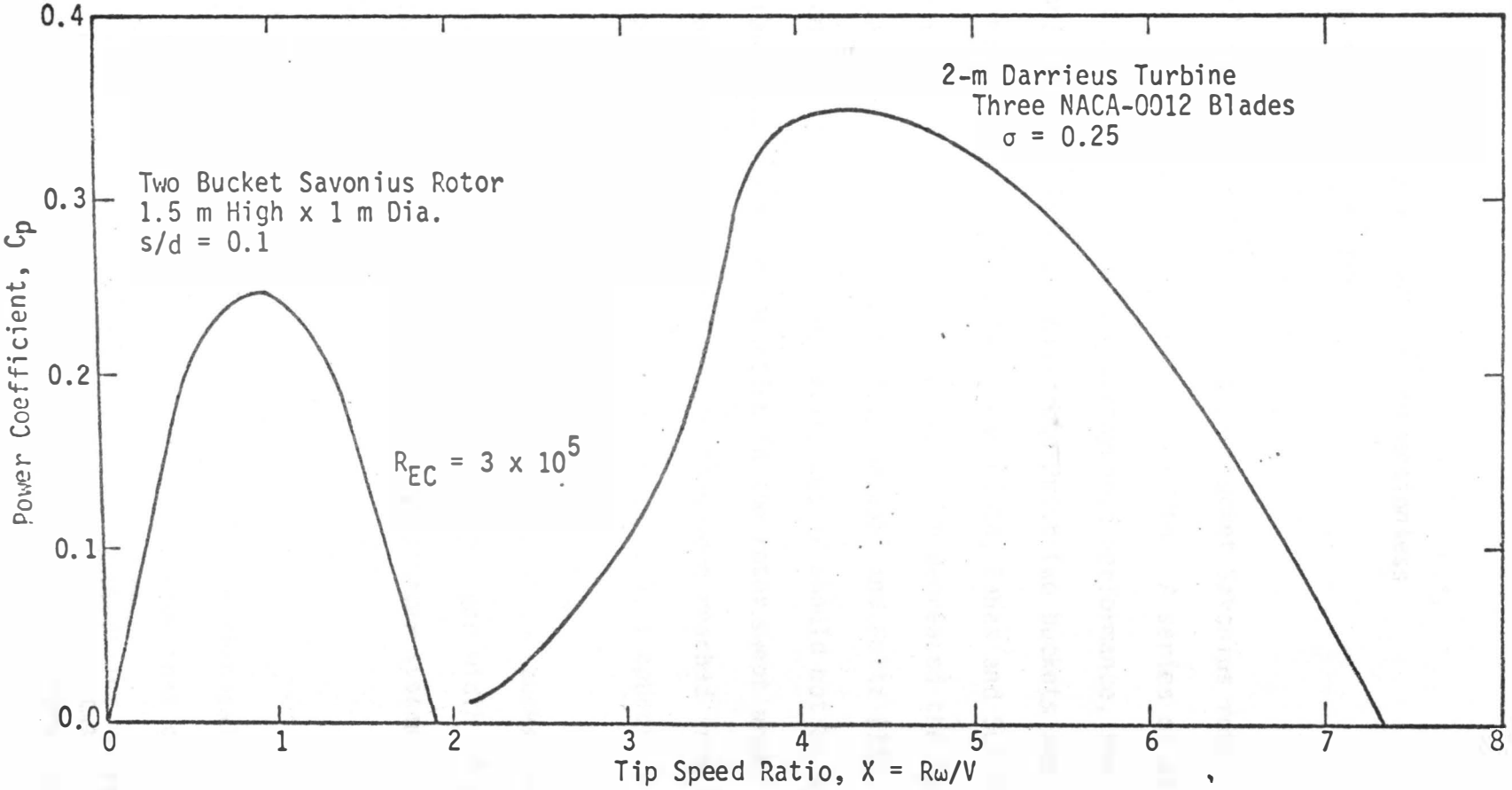

Figure 16. Comparison of Performance Curves for a Two-Bucket Savonius Rotor and a Three-Bladed Darrieus Wind Turbine, at Identical Reynolds Number, $R_{EC} = 3 \times 10^5$

From Banas et al. (1976)

is defined as:

$$\text{gap width} = \frac{s}{d}, \text{ dimensionless} \qquad (22)$$

where s = actual gap width, m

d = bucket diameter, m

Figure 17 depicts a schematic of a two bucket Savonius rotor with 180^{o} buckets and illustrates the bucket gap width. A series of wind tunnel tests indicate that, for better aerodynamic performance, the most efficient configuration is a Savonius rotor with two buckets and a small gap opening between the buckets or gap width, Banas and Sullivan (8). Savonius (45) also realized that a gap width decreased the rotor drag and increased its speed. Blackwell, Sheldahl and Feltz (13) reached the conclusion that some gap is desirable, but it should not be so large that it will cause considerable reduction in the rotor swept area, A, and radius of rotation, R. The following conclusions were reached from the study:

1. A dimensionless gap width of s/d = 0.10 to 0.15 appears to yield optimum performance.
2. The recommended configuration is two sets of two bucket rotors rotated 90^{o} apart, with each rotor having a gap width of s/d = 0.1 to 0.15 to be utilized as a passive starter system for a Darrieus wind turbine.

Heat Pump

A heat pump can be defined as a reversible mechanical air conditioning system or mechanical refrigeration system that can both heat or cool. This dual feature is accomplished by reversing valves that change the direction of the refrigerant flow. Both systems utilize a

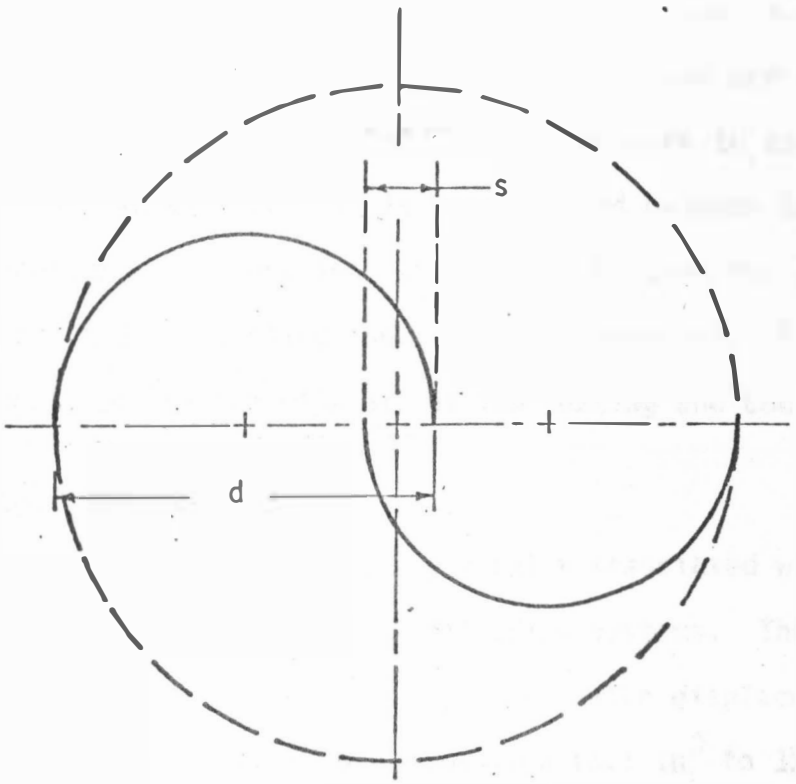

Figure 17. Schematic of the Two-Bucket Savonius Rotor with 180° Buckets.

From Blackwell et al. (1977)

compressor, condenser, cooling coils or evaporator, throttling valve, controls, and necessary piping for heating or cooling, Ambrose (1).

When a heat pump is operating as a heating system, the heat is usually taken from outdoor air, water, the ground, the solar energy, or other heat source and delivered together with the heat equivalent of the compressor work to the system. When the heat pump is operating as a cooling system, it exhausts heat from the system and rejects it together with the heat equivalent of compressor work to an outside sink. The heat exchange process is accomplished between the evaporator and the condenser. When heating, the process is from the evaporator to the condenser, and for cooling the process is reversed. Figure 18 shows a typical heat pump system with air as the heating and cooling medium.

Variable Speed Compressor

Variable speed compressors are generally associated with vehicles, particularly with automobile air conditioning systems. The compressors utilized today have from two to six cylinders with displacements ranging from 100 ml to 207 ml per revolution (6.1 in^3 to 12.6 in^3 per revolution), ASHRAE (3). The compressor draws power directly from the engine in the follwoing two ways: directly from the engine crankshaft to the compressor crankshaft via V-belts and sheaves, and indirectly as electrical energy from the battery, which operates the electromagnetic clutch and other necessary electrical control devices. Variable speed automobile compressors are divided in two categories: The piston or reciprocating compressor and the rotary compressor.

The existing automobile piston type air conditioning compressor

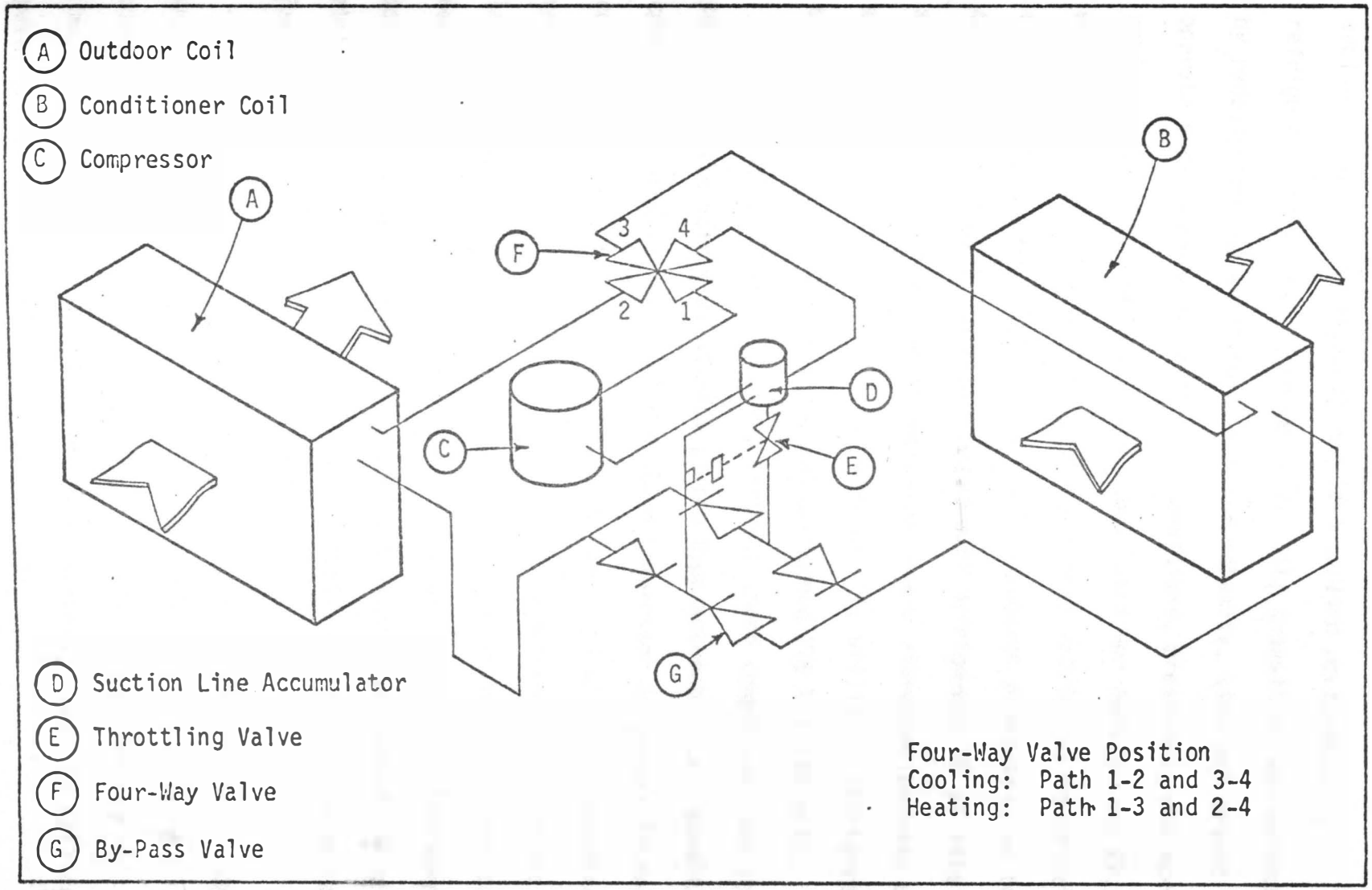

Figure 18. Heat Pump System with Air as Heating and Cooling Medium

From Ambrose (1966)

evolved from the conventional vertical in-line reciprocating refrigeration compressor, Holmes (29). The transition was accomplished by redesigning the existing compressor capacity, size and weight to operate under widely variable load conditions, pressures, and speed ratios. Also, Refrigerant 12 was substituted for Refrigerant 22, which was used in the past to gain additional refrigerating effect for a given displacement, ASHRAE (3). High discharge pressures, up to 4480 kPa (649.8 psi), were associated with Refrigerant 22 at idle and slow automobile speeds, which generated severe vibration pulses, and also accentuated compressor seal problems. By utilizing Refrigerant 12 the pressures at idle conditions seldom exceed 276 kPa (40 psi).

In recent years, the rotary, variable speed compressor has started to replace the more conventional piston type automobile air conditioning compressor. The rotary, variable speed compressor is generally more compact in size than reciprocating compressor and utilizes rotating vanes to compress the refrigerant gas. The compressor can provide large cooling capacity for a wide variety of vehicles, including trucks, recreational vehicles and farm and off-highway equipment. The compact design can also provide greater mounting flexibility, reduced weight, minimum noise and vibration problems, and this compressor system has fewer parts, Anonymous (2).

The capacity of a compressor is a function of two factors: speed and actual effective displacement. Actual effective displacement is expressed as a specific quantity of refrigerant circulated per unit of time and depends on the compressor's bore, stroke, number of cylinders, speed, and volumetric efficiency, Holmes (29).

Stable operation of automotive air conditioning system depends upon the performance and interaction between the individual components of the system over the full range of operating conditions, Newton (38). The following information is needed for an idealized system analysis:

1. The complete range of compressor performance characteristics for all speeds at which it will be driven, corresponding to respective suction pressures and discharges pressures.
2. The performance characteristics of the evaporator for all expected air quantities, temperatures, and refrigerant evaporating temperatures.
3. The complete performance characteristics of the condenser over the full range for the air quantity, the refrigerant mass flow from the compressor, refrigerant condensing temperature and degree of subcooling.

Newton (38) notes that an actual system will depart from the idealized system analysis due to:

1. Pressure drop in the suction and discharge lines.
2. Pressure drop within the evaporator and condenser.
3. Unequal feeding of the refrigerant in the evaporator or condenser.
4. Non-uniform air velocity distribution over the evaporator and condenser.
5. Superheat throttling range of the expansion valve.
6. Oil pumping level of the compressor.

Wind Turbine Operational Systems

Wind energy operational systems for a wide variety of applications

can be divided into two general classes: constant and variable rotational speed systems. The constant speed systems, utilizing the Darrieus wind turbine in conjunction with electric systems, have received vast coverage, but variable speed systems, smaller in numbers, have received relatively little coverage, Banas and Sullivan (7).

The basic elements of the constant speed system, used for generation of electrical energy that is introduced into a utility grid, are shown in Figure 19. A turbine rotating at constant speed is connected to a synchronous generator through a fixed gear-ratio speed increaser. The generator is connected to an electrical power network, which determines the synchronous frequency. This can be accomplished, if the network capacity is large relative to the wind energy system, Banas and Sullivan (8). ASME (4) notes that wind machines, when operated at constant rotor speeds can waste as much as 75 percent of the available wind energy, when contrasted with variable rotor speeds. Thresher and Wilson (54) conclude that at a fixed RPM, higher wind speeds decrease the tip speed ratio, which in turn results in lower power output at wind speeds above the rated speed.

Ramakumar (40) and Jayadev (31) characterize a variable speed system as allowing the turbine rotational speed to vary optimally with wind, corresponding to a tip speed ratio that will maintain a high coefficient of performance, C_p, for a given wind turbine. Applications of variable speed systems include water pumping for irrigation and direct current generator, regulator storage combinations for generation of electricity in remote areas, Blackwell et al. (15). For generating electric power with a variable speed rotor, the aeroturbine speed is

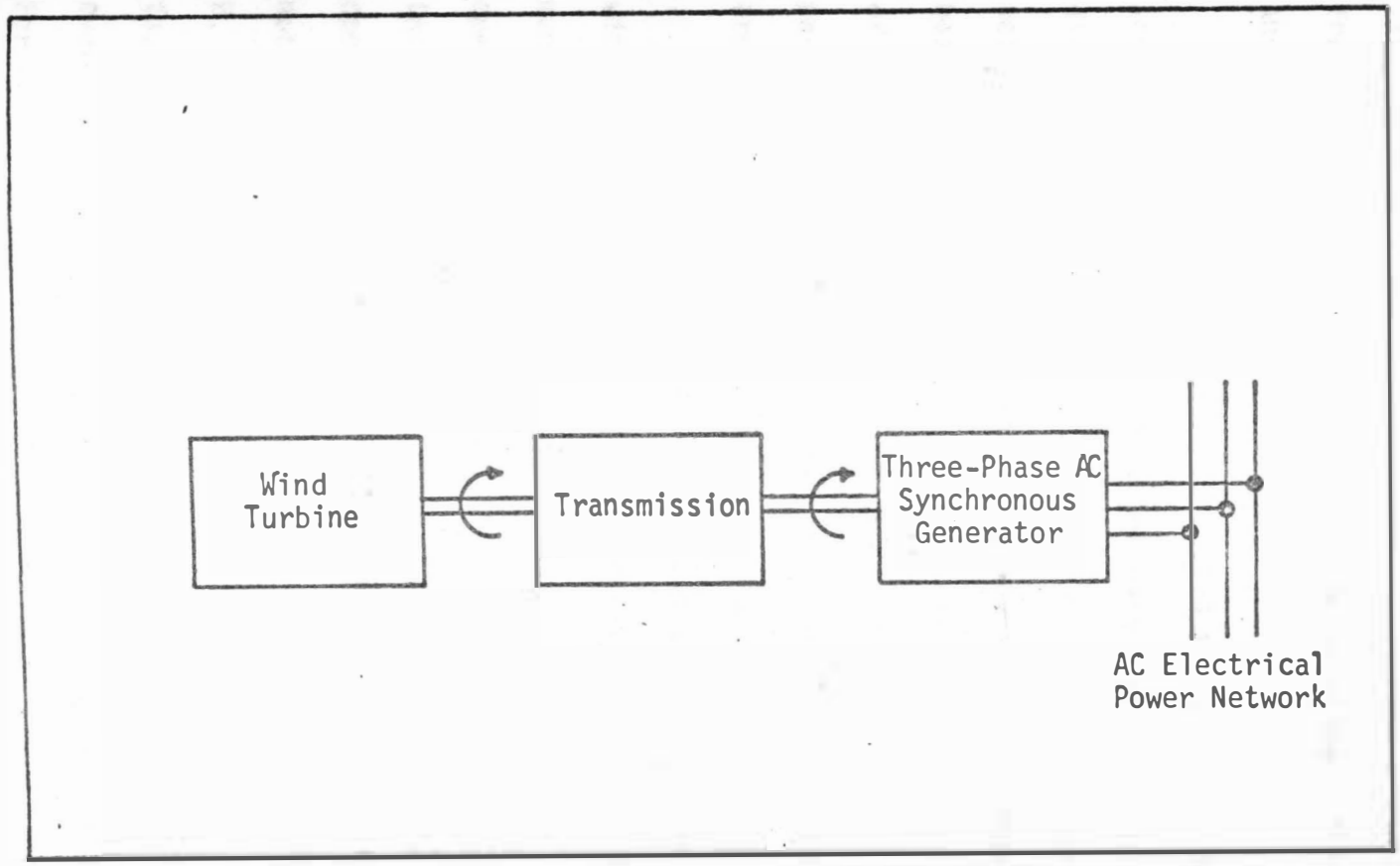

Figure 19. Synchronous System Diagram.

From Banas and Sullivan (1976)

allowed to vary optimally with wind speed and the system utilizes a variable speed, constant frequency generating system to obtain constant frequency power which is sent into an existing utility grid, Ramakumar and Hughes (41), and Jayadev (31).

A better understanding of variable speed performance can be accomplished by noting the system torque characteristics. Figure 20 displays the relationships between torque, rotor speed and wind velocity for a Darrieus wind turbine. The performance curves shown are based on a maximum diameter of 5 m (15 ft), a height to diameter ratio of one, three blades, a blade chord of 190.5 mm (7.5 in), and a parabolic blade shape. Superimposed on the turbine performance curves are three possible speed dependent loads A, B, and C.

Since, theoretically, a Darrieus turbine is not self-starting, with load A the system will not operate because the load torque requirement always exceeds the turbine torque capability. If a fixed-ratio speed increaser is inserted between the turbine and the output device, the load characteristic is shifted from A to C. The system will operate with load C, but the maximum torque capability of the turbine is not realized. When a speed increaser ratio is selected to obtain load B, the selection appears to represent an optimum, as it is very close to, but less than, the maximum torque capability of the turbine. However, transient wind speed variations can lead to problems with load B. For example, if the system is operating at a stable point corresponding to a wind speed of 4.4 m/s (10 mph), a sudden gust to wind speeds above 6.7 m/s (15 mph) results in a reduction of turbine torque, hence a reduction in turbine RPM. Should the wind speed remain above 6.7 m/s

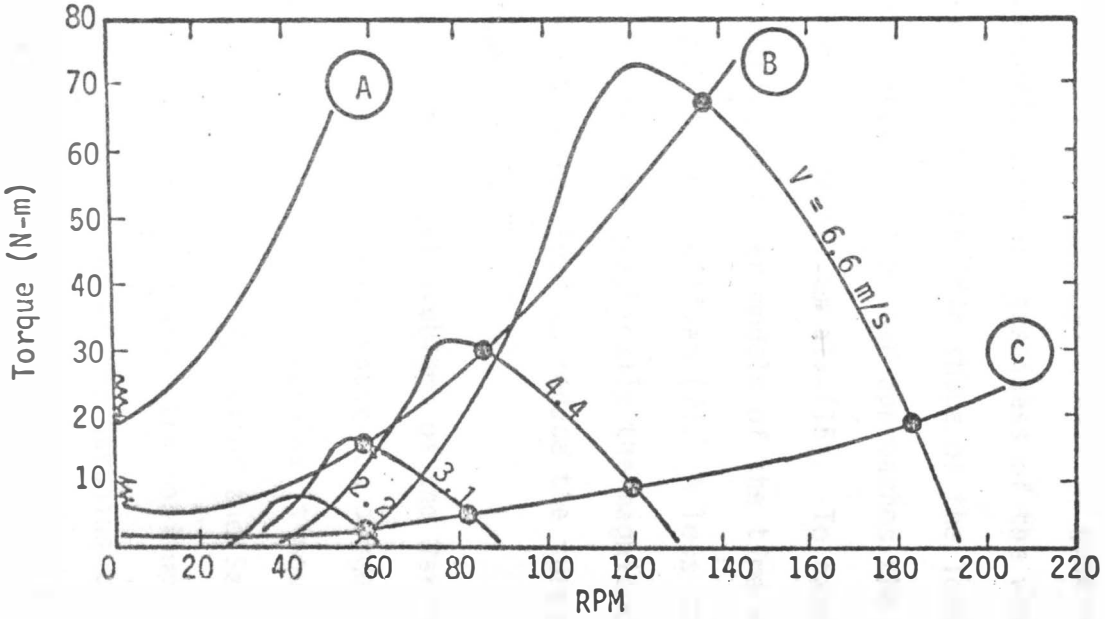

Figure 20. Performance Characteristics of a Darrieus Turbine and Speed-Dependent Loads (1 m/s = 2.27 mph, 1 N-m = 0.74 ft-lbf).

From Blackwell et al. (1977)

(15 mph) the system will continue to slow down until it stops. If the turbine slows enough during the transient period, the wind speed could return to 4.4 m/s (10 mph) and the turbine speed would still continue to decrease. This stalling effect is difficult to generalize, because it depends on many factors, such as, gustiness of the wind environment, the system inertia, and the specific shape of the load curve. The problem becomes more acute as the load approaches the maximum torque output of the turbine, Blackwell et al. (15). To examine the stalling problem more completely, computer models of the time response of the turbine are useful, Banas and Sullivan (7). A less complex approximate approach is to determine graphically the magnitude of the smallest step change in wind speed required to reduce the turbine torque to less than the load torque.

To decrease the operational problems of the Darrieus turbine, a combination of Darrieus and Savonius rotor was suggested, Blackwell (10), Banas and Sullivan (7). The Savonius turbine is mounted on the same shaft as the Darrieus turbine. The radius of the Savonius turbine is selected such that both turbines achieve the maximum efficiency at the same rotational speed. The height of the Savonius turbine is selected to be one-half the height of the Darrieus turbine. Figure 21 shows a Darrieus-Savonius turbine combination with three superimposed loads A, B, and C. The Darrieus size configuration corresponds to the previous example. Figure 21 is only approximate in that the separate torques from each turbine are summed while neglecting potential interference effects. The most notable feature is that starting torque is now available. Once started, load A can be maintained, although the system

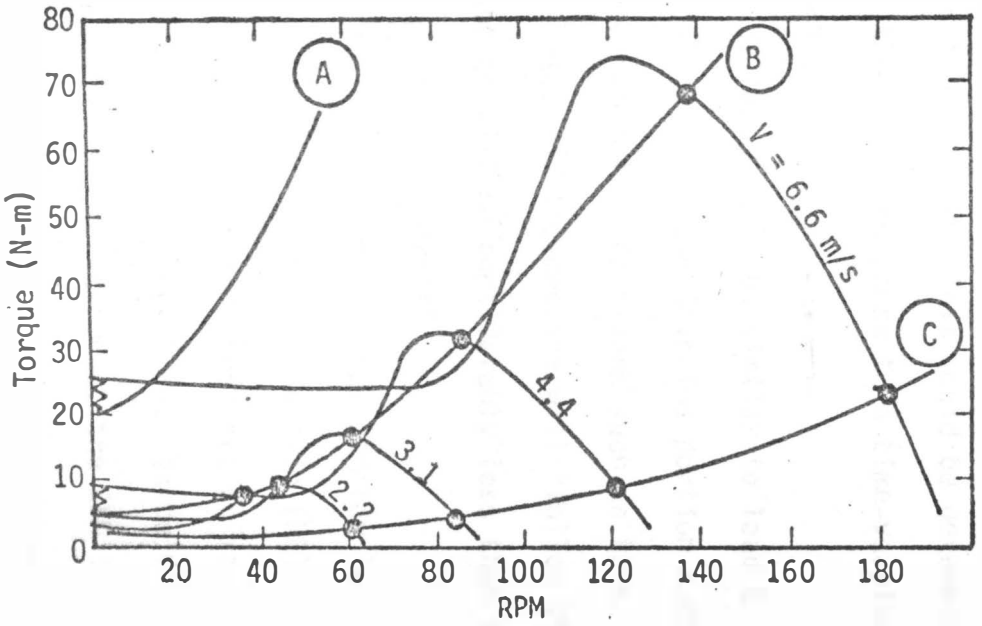

Figure 21. Performance Characteristics of a Savonius Assisted Darrieus Wind Turbine and Speed-Dependent Loads (1 m/s = 2.27 mph, 1 N-m = 0.74 ft-lbf).

From Blackwell et al. (1977)

will operate only on the Savonius portion of the curve.

For load B, the Savonius portion can alleviate the stalling problem discussed previously. Rather than stalling, the system will tend to operate on the Savonius part of the curve. The exact analysis of which equilibrium points on the curve are followed in a wind environment is a complicated problem. This could be determined with a real-time modeling of the system response to a time-varying wind velocity, Banas and Sullivan (7).

Performance of load C will be similar to load C operating with a Darrieus turbine alone, with the Savonius portion contributing to starting from zero RPM only. For loads such as this, gust stalling tends to be eliminated and the machine will "follow the wind", although the energy extraction will be considerably less than is potentially available from the Darrieus turbine.

The problem of limiting the maximum RPM for loads B and C still exists for variable speed operation. Templin (52) has experimented with centrifugally controlled blade spoilers or variable blade flaps to regulate maximum RPM. Another possibility is to fit the load such that it reaches the maximum turbine torque at the RPM limit. As of now, adequate designs with variable speed operation have not yet evolved, Banas and Sullivan (7), Blackwell et al. (15).

Operational Characteristics of Constant-Speed Systems

A constant-speed load system can be implemented by connecting a turbine rigidly through a fixed-ratio speed increaser to a synchronous generator. The generator is typically connected to a utility grid

capable of maintaining constant frequency. System operation is maintained as long as the pull-out torque rating of the electrical machine is not exceeded. Performance characteristic of a 5 m (15 ft) diameter Darrieus turbine and a constant speed load are shown in Figure 22. The important feature is that with proper sizing the load rating will never be exceeded for any wind speed. Therefore, no spoilers or other speed limiting mechanisms are needed for the turbine, Blackwell et al. (15), Banas and Sullivan (7).

Vertical Axis Turbine Cable Tie-Down System

Most vertical axis wind turbine systems have incorporated the cable tie-down design, Banas and Sullivan (8), South and Rangi (48), Templin (52), Clark and Scheider (19), Simonds and Bodek (46), Chasteau (16), Maile (37), and Hagen (27), as opposed to the cantilevered, unguyed system. Guy cables, directed from ground locations to a point atop the turbine rotor, are thought to provide lateral stability of the wind conversion system against the steady and transient, overturning loads caused by the wind.

Several problems can arise, if the cables are not properly selected and pretensioned, Reuter, Jr. (43), Clark (18), Hagen (27). A specific number of cables must be selected to ease turbine erection, provide uniform polar support and minimize wind blockage. Proper cable size and material must be selected to control tower deflection and tension changes. Also, initial tensions in the cables must be selected to minimize cable sag to provide rotor support, and to eliminate cable vibrations at normal turbine operating ranges.

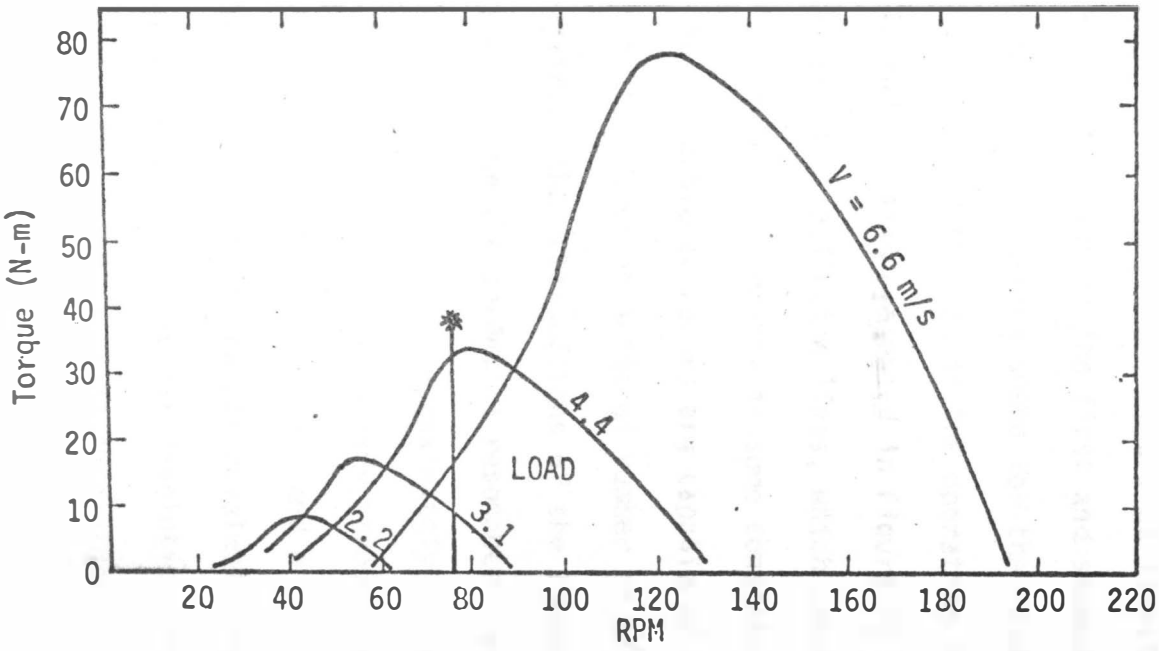

Figure 22. Performance Characteristics of a Darrieus Turbine and a Constant-Speed Load (1 N-m = 0.74 ft-lbf, 1 m/s = 2.27 mph).

From Blackwell et al. (1977)

The wind turbine blade loadings, that include centrifugal, gravitational and aerodynamic forces, can set up blade deformations or blade flap modes with corresponding natural frequencies, Banas and Sullivan (8), Blackwell et al. (15). Figure 23 illustrates how the calculated natural frequencies of the first and second normal blade bending modes depend on the turbine speed for the Sandia 5 m (15 ft) Darrieus vertical axis wind turbine in the operating angular velocity range of 10 to 40 rad/s. Also presented in Figure 23 are constant slope lines or number per revolution lines, which represent the loci of points where the natural frequency is some constant multiple of the turbine speed. Multiple bladed rotors are capable of reacting to oscillatory forces that occur an integral number of times in one revolution. Therefore, the intersections of the lines with natural frequency curves determine the potential resonance areas. Wind turbine study shows that at speed ratios of approximately three and above, normal, aerodynamic forces on one blade vary through one cycle in each turbine revolution, Banas and Sullivan (8), and a wind turbine with three blades, each loaded by this one per revolution excitation at 120^{o} phase angles will experience a three per revolution excitation. Figure 23 illustrates the potential resonance areas at approximately 15 rad/s and 2 rad/s angular, rotor speeds for a three-bladed rotor.

When calculating blade frequencies, turbine components cannot be treated independently. The elastic nature of the turbine blades and rotor tube suggests that motion in one component will induce motion in the other. Also, coupling effects among the system components, such as the rotor and the transmission, can change component resonant

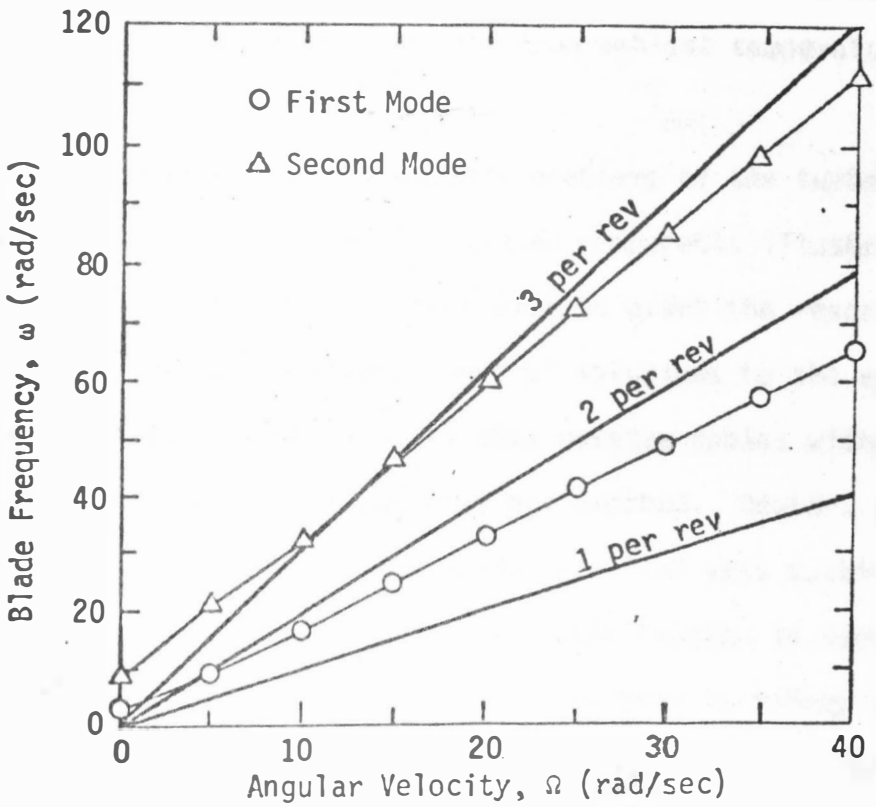

Figure 23. Natural Frequency Spectrum (first two modes), ω, versus Angular Velocity, Ω, for Darrieus Wind Turbines.

From Banas and Sullivan (1976)

frequencies and introduce additional vibration modes, Blackwell et al. (15).

Tie-down system cable frequencies vary as the square root of the cable tension, Reuter, Jr. (43), so that initial cable tension is closely associated with the location of cable natural frequencies. Also, initially tensioned cables will not have a constant value but will change due to cable relaxation, and from ambient temperature and insolation changes.

The cited combined natural frequency problems of the turbine blades, cables, and other wind energy system components illustrate the need for frequent "tuning" of the cables to avert the resonances for turbine cable tie-down systems. Several solutions to the existing problems are possible. Hagen (27) utilizes massive cables with low tension so only the harmonic frequencies are excited. Reuter, Jr. (43) suggests that for a higher speed two-bladed vertical axis turbine, it may be more desirable to lower the initial cable tension in such a way that the two per revolution frequency of the turbine is midway between the first two cable modes. Banas and Sullivan (8) describe a conservative approach for a three-bladed Darrieus vertical axis wind turbine, by raising the lowest flap resonant frequency above the three per revolution line.

Wind Energy Economics

Since wind energy offers several alternatives for agricultural applications, those processes which are used the greatest number of days will be the most economical. These will produce the greatest

yearly amount of energy per unit of power, therefore, yielding the fastest economic return for the system. Also capital intensive wind energy systems with high annual usage are likely to be more economical, other factors being equal, Liljedahl (36).

Agricultural wind energy applications which are used predominantly in areas of high average winds or those used predominantly in seasons of high average winds are also likely to be more economical. This is due to the fact, that needed wind energy can be captured with a smaller machine, which reduces the needed capital investment and reduces the break even cost of conventional energy with which it must compete, Liljedahl (36).

A simple method for determining the cost of energy for a horizontal axis, wind turbine, electric generator system can be determined from the average power density at a specified turbine height and location. The total yearly energy is the product of the average power density (related to the effective height of turbine, and anemometer height), the turbine swept area, and the total yearly period of operation. Dividing the total yearly energy by the total capital investment determines energy per dollar investment. The desired rate of return then determines the cost per energy. Also the effective turbine height can be adjusted to determine if the change in average power density will offset the corresponding change in tower cost, and rated wind speed can be adjusted to maximize the average generated power, Johnson (32).

The annual turbine wind energy can also be determined by using the load factor for a horizontal axis wind turbine electric generator

system, Swift, Jr. (51). Load factor, L.F., is defined as the fraction of energy that a given wind turbine produces over a specified time interval, as compared to the total energy that the machine would produce, if it operates at rated capacity continuously over the same period.

$$\text{L.F.} = \frac{\text{average power}}{\text{rated power}} \tag{23}$$

Therefore, the annual turbine wind energy is the product of rated energy, load factor, and total yearly period of operation. The annual cost of the machine, including interest charges, taxes, depreciation, operation and maintenance can be calculated as a function of the total capital cost.

$$\text{Annual Cost} = \text{Capital cost} \times \left(\frac{\text{percent}}{\text{total annual charges}}\right) \tag{24}$$

The cost per unit of energy is obtained by dividing the annual cost by annual wind turbine energy.

Templin and South (53) relate the cost of increased power to the rotor center height and the turbine swept area for a vertical axis wind turbine. The turbine rotor height will be optimum when the cost of obtaining a unit gain in average power by increasing the height is the same as the cost of obtaining the same increase by enlarging the swept area.

Weingarten and Blackwell (56), Banas (5), Banas and Sullivan (8) conclude that economics of wind power generation systems involves a complex interplay of both cost and performance parameters. Blade cost and transmission cost are the two major contributors to the total system cost. Blade cost can be related to the swept area of the turbine, and transmission cost related to output torque of the turbine. Therefore,

it is reasonable, that annual energy cost can be related to the turbine swept area and turbine transmission. Insofar as these economic indicators are relatively easy to evaluate, a wide range of postulated systems can be analyzed.

DEVELOPMENT OF PROPOSED SYSTEM PERFORMANCE CURVES

The performance characteristic curves for the proposed variable speed wind turbine-compressor system are developed by regression analysis using data from a similar, existing set of variable speed wind turbine torque performance curves for a wider range of required wind speeds. The regression coefficients so determined were used to develop the prediction curves for the proposed system. This procedure was utilized due to scarcity of data for the proposed system.

The needed Savonius-Darrieus combination wind turbine torque curves will be similar to the existing wind turbine system curves which have been shown and described in Figure 21. The systems have similar configuration in that, both have identical 5 m (15 ft) blades, height to diameter ratios of unity, and NACA-0015 (National Advisory Committee for Aeronautics) symmetrical airfoil shapes.

The differences exist between chord lengths, maximum coefficients of performance, ($C_{p_{max}}$), and the maximum tip speed ratios, X_{max}. The existing turbine has a chord length of 190.5 mm (7.5 in), maximum coefficient of performance, 0.36, and maximum tip speed ratio of 4.7. The proposed turbine has a chord length of 152.4 mm (6 in), maximum coefficient of performance, 0.35, and maximum tip speed ratio of 5.0. Due to these turbine configurations, the existing turbine blades have a higher solidity than the proposed system blades. Since the existing torque performance diagram has constant wind speed curves ranging from 2.2 m/s to 6.6 m/s (5 mph to 15 mph), there exists a need to extend the constant wind speed curves to include the rated and furling wind speeds.

Curve fitting is utilized by drawing curves, and straight lines intersecting the existing Savonius-Darrieus Torque performance curves of Figure 21 at such points as the peaks, transition areas between the Savonius and Darrieus curves, and at near zero torque areas. The possible curve fits for the drawn curves are a straight line ($y = a + bx$), an exponential curve ($y = ae^{bx}$), a power curve ($y = ax^{b}$) and a logarithmic curve ($y = a + b\ln x$). By doing regression analysis, the constants a and b are obtained and the spacing for the projected constant wind speed curves is obtained. The resulting torque data of the projected and fitted curves are converted to the power data by equation (5) and the projected power characteristic curves of the proposed Savonius-Darrieus wind turbine system are drawn as indicated in Figure 24.

Compressor power input curves for 100.0 cm^3/Rev (6.1 in^3/Rev), 142.6 cm^3/Rev (8.7 in^3/Rev), and 168.8 cm^3/Rev (10.3 in^3/Rev) displacements were obtained from the manufacturer and were superimposed on the turbine power curves. The expected performance of the system is defined at the intersection of the constant wind speed and the compressor curves.

DESIGN PLAN

The proposed system utilizes the cantilevered unguyed tie-down concept in conjunction with a three-bladed Darrieus rotor for minimizing wind induced thrust loads, and system vibrations. The non-articulating Savonius-Darrieus variable speed compressor wind energy conversion system essentially, consists of the rotor assembly, tower structure,

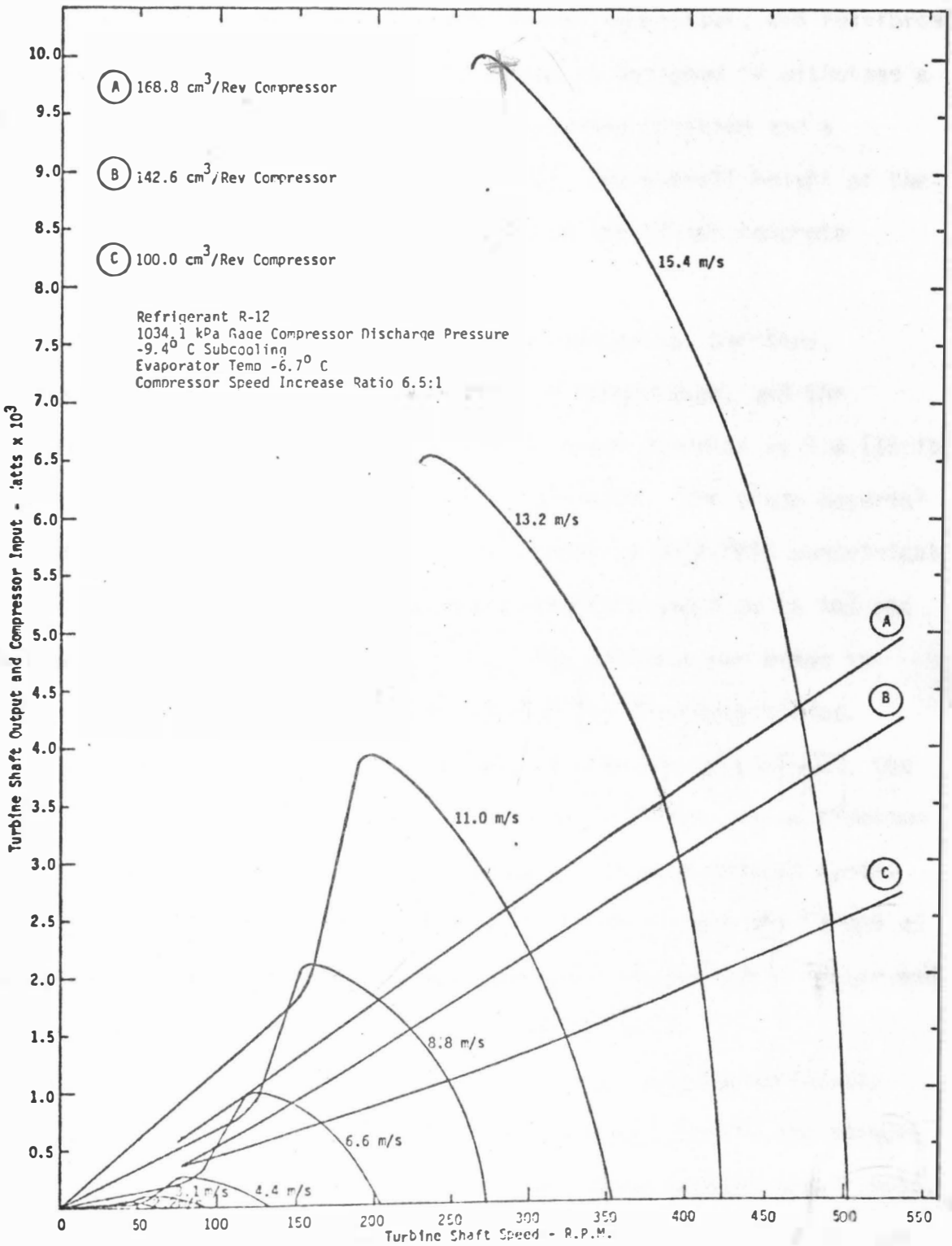

Figure 24. Performance Characteristics of a Hybrid Darrieus-Savonius Wind Turbine and Speed-Dependent Loads for 168.8, 142.6 and 100.0 cm³/Rev Reciprocating Compressors at Constant Wind Speeds (m/s).

bearing supports, brake assembly, belt driven compressor, and reinforced concrete foundation, Figure 25. The system is designed to withstand a 44 m/s (100 mph) survival wind speed in a parked position and a 19.8 m/s (45 mph) wind speed while running. The overall height of the system is 8.3 m (27.3 ft), measured from the top of the concrete foundation.

The rotor assembly consists of non-articulating, Darrieus, troposkien airfoils, two Savonius rotors, a torque tube, and the Darrieus blade attachment. The troposkien blade diameter is 5 m (15 ft), with an airfoil height to diameter ratio of unity. The blade material is a lightweight extruded aluminum alloy, with an NACA-0015 symmetrical airfoil cross-section. The blade chord length is 152.4 mm (6 in) and the maximum tip speed ratio, X_{max} is 5. The solidity per blade is 0.067, which equals a total solidity of 0.2 for the three blades.

The turbine torque tube, which supports the Darrieus blades, the Savonius rotors, and the large compressor drive sheave, is an aluminum schedule 120 pipe, and is designed to resist the wind induced cantilevered moments, thrust loads, aerodynamic loadings, and the torque of the turbine rotor. The torque tube has a 168.3 mm outside diameter and a 14.3 mm thick wall (6 5/8 in O.D. x 0.562 in wall).

To minimize the starting and the wind gust stalling difficulty of the Darrieus rotor, two Savonius rotors are attached to the torque tube, close to the upper and the lower ends of the turbine torque tube, Figure 25. The end plates and buckets of the Savonius rotors are constructed of 6.4 mm (0.25 in) thick aluminum plates. The height of each Savonius rotor is 114.3 cm (45 in) with the projected width of each

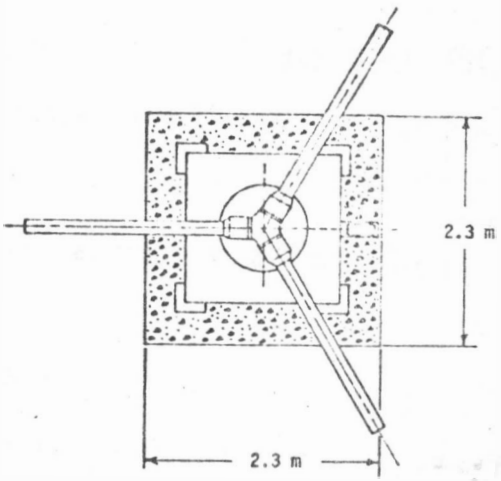

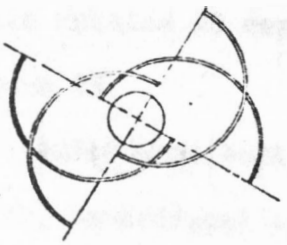

Section A-A

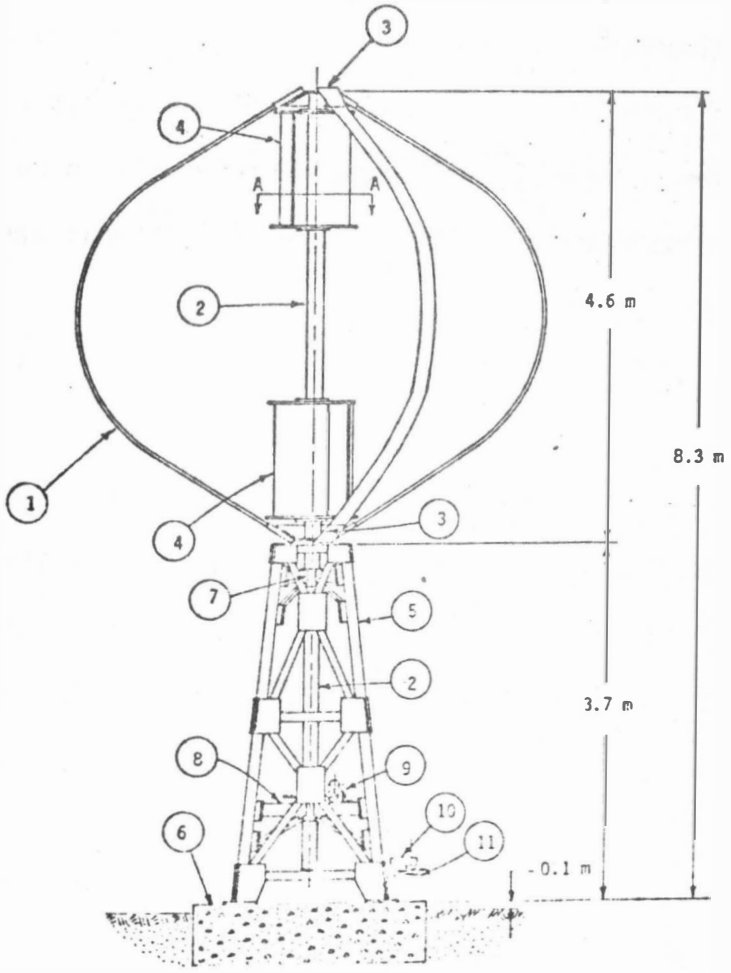

	Description
1	Airfoil
2	Torque Tube
3	Airfoil Attachment
4	Savonius Rotor
5	Tower
6	Concrete Pad
7	Upper Bearing Support
8	Lower Bearing Support
9	Caliper Disc Brake
10	Air Conditioning Compressor
11	Compressor Drive

Figure 25. 5-m Darrieus Vertical Axis Wind Turbine System

rotor being 81.3 cm (32 in), Figure 26. To ensure the self-starting of the Darrieus rotor for any initial wind direction, each rotor has two buckets, and the buckets of the upper rotor are rotated 90 degrees from the buckets of the lower Savonius rotor, Figure 25.

The Darrieus blade attachment is designed to resist wind buckling forces at 55 m/s (125 mph) in a parked position, and centrifugal and aerodynamic forces of the rotor at 26.4 m/s (60 mph) wind speeds. The blade attachment consists of a 6.4 mm (0.25 in) thick aluminum terminal plate and 38.1 mm (1.5 in) thick split clamp, Figure 27. The split clamp consists of two 19.1 mm (0.75 in) thick aluminum clamp plates into which the airfoil shape is cut. The halves are brought together to clamp the blade end securely. A 76.2 mm (3 in) tapered section at the outer end of the clamp plate halves is provided for a transition of stress from the blade into the solid section of the clamp. Each blade split clamp is fastened to each terminal plate end with six 9.5 mm (0.375 in) diameter, anodized, aluminum bolts.

The rotor assembly and torque tube are located at the top of a 3.7 m (12 ft) rectangular, four-sided tower structure. The tower structure is 1.5 m (5 ft) square at the base and tapers to 0.8 m (2.5 ft) square at the top, Figure 25. The tower is a portable steel, welded-bolted structure consisting of angle irons and steel plates. The tower column material is 101.6 mm x 101.6 mm x 7.9 mm (4 in x 4 in x 5/16 in) angle, side brace material is 88.9 mm x 88.9 mm x 7.9 mm (3 1/2 in x 3 1/2 in x 5/16 in) angle, and diagonal material is 76.2 mm x 76.2 mm x 6.4 m (3 in x 3 in x 1/4 in) angle. The tower is reinforced in the corners and at truss joints by 4.8 mm (3/16 in) steel plates.

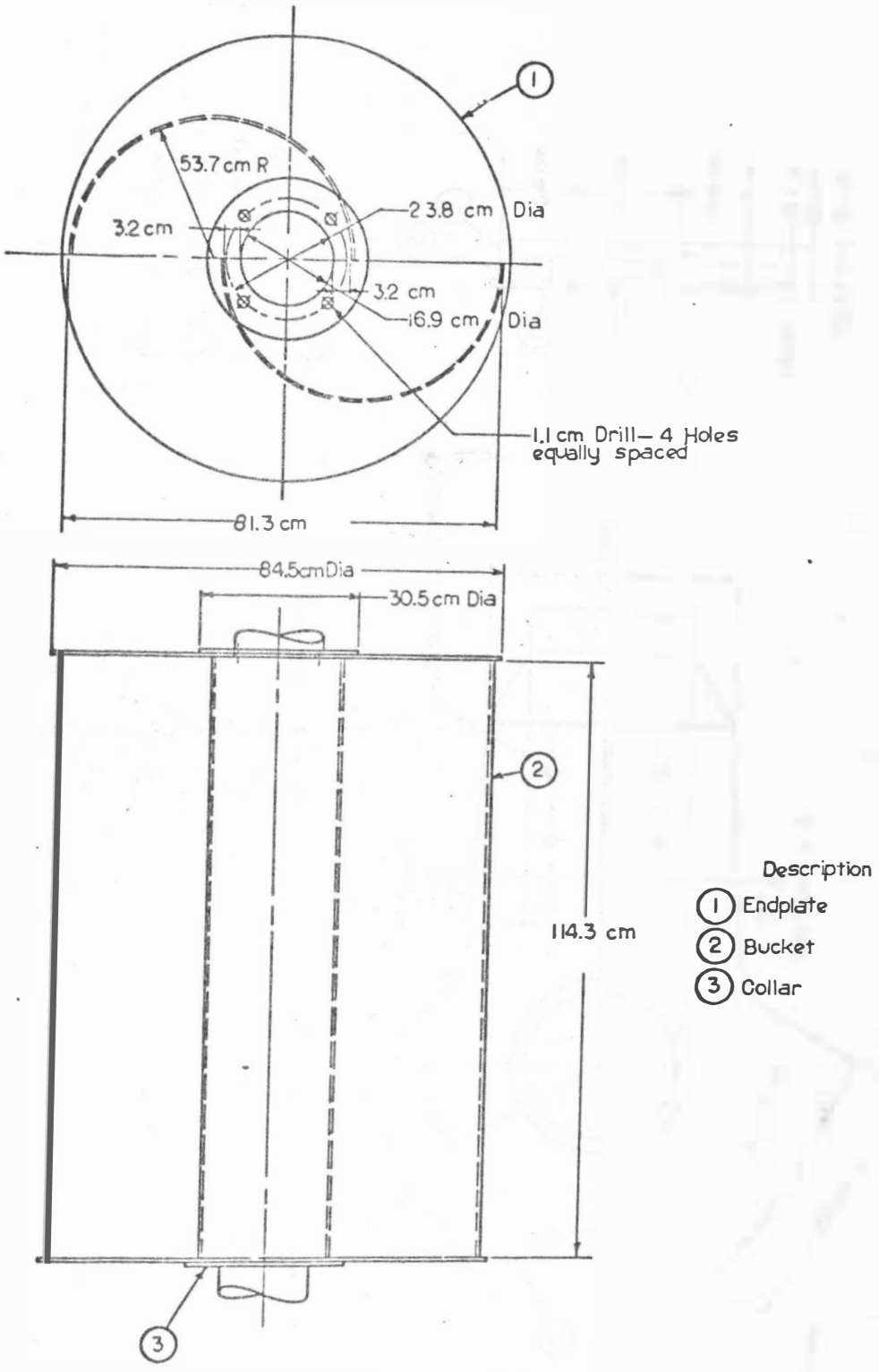

Figure 26. Savonious Rotor

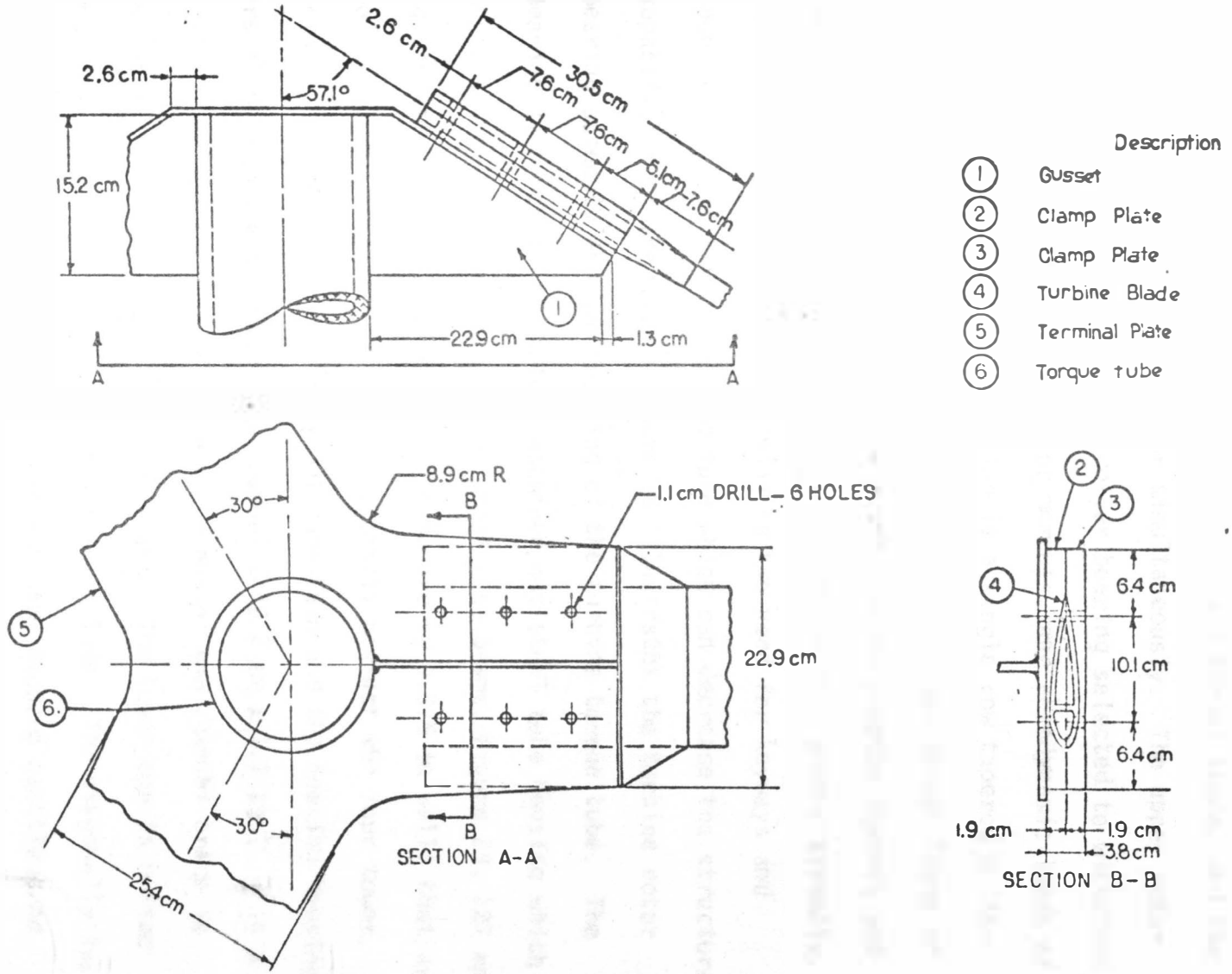

Figure 27. Turbine Blade Attachment

The turbine rotor bearings are tapered roller, grease lubricated which are adapted to minimize the radial, and thrust loads, and the misalignment of the turbine rotor simultaneously. The upper rotor bearing is a double row tapered roller bearing selected to withstand the severe wind cantilevered rotor moments, and aerodynamic loads of the rotor. The lower rotor bearing is a single row tapered roller bearing selected to primarily resist the radial and thrust loads of the rotor. The bearings are mounted on tapered adaptor sleeves and secured to the torque tube with a lock nut and lock washer assembly. The adaptor sleeve mounting eliminates the need for keyways and shoulders on the turbine torque tube which can decrease the structural capabilities of the tube. Figure 28 illustrates the turbine rotor bearing assembly and the mounting of the turbine torque tube. The bearing is press fitted into a machined out steel tube housing which is supported by four diagonal square steel tube beams, Figure 29, 127 mm square with 9.5 mm thick walls (5 in square by 0.375 in wall) that are bolted to and abut on the inside diagonally against the four tower columns. Each support arm or steel tube beam and the bearing housing are also braced underneath by a channel C 76.2 mm x 1.9 kg (C 3 in x 4.1 lb) structural section. The upper end of the channel brace is welded to the bearing and the support arm. The lower end is bolted and abuts on the inside against the tower column. The diagonally supported bearing structure will resist the wind induced cantilevered moments and tension of the housing and the tower. Thus bolt loading will consist primarily of shear and compressive forces. Figure 25 illustrates the mounting of bearing housing support assemblies.

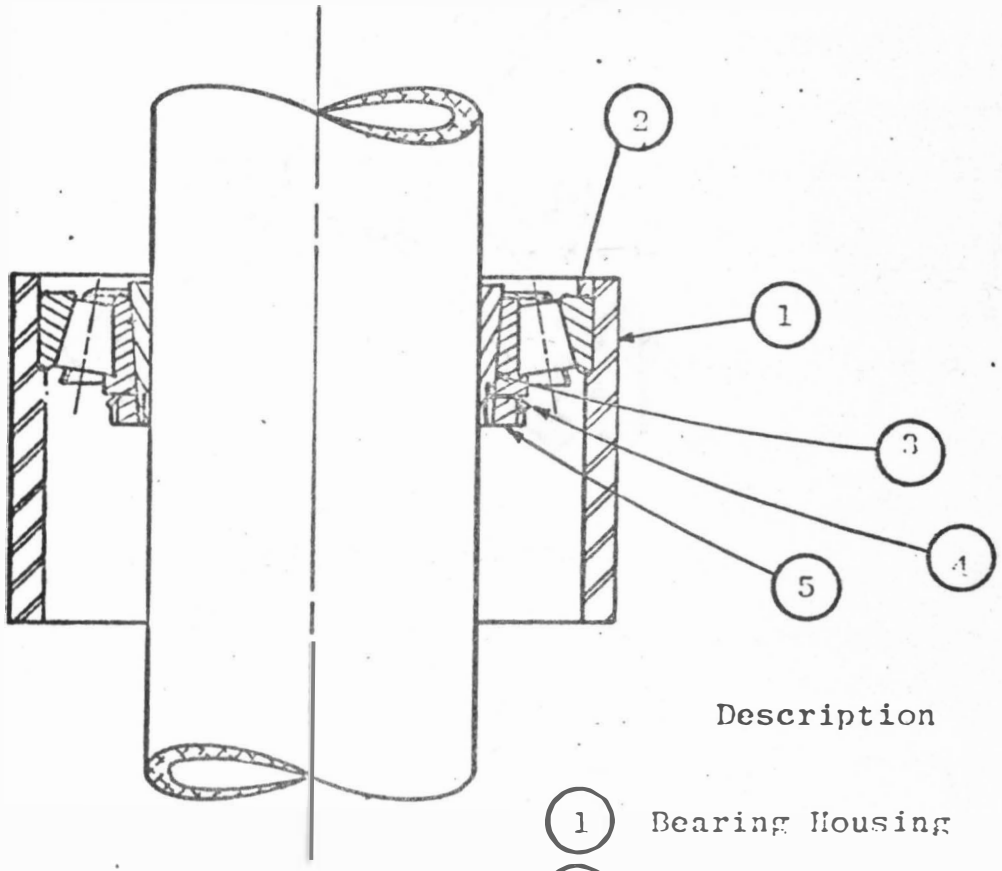

	Description
1	Bearing Housing
2	Tapered Roller Bearing
3	Adaptor Sleeve
4	Lockwasher
5	Locknut

Figure 28. Turbine Rotor Bearing Assembly

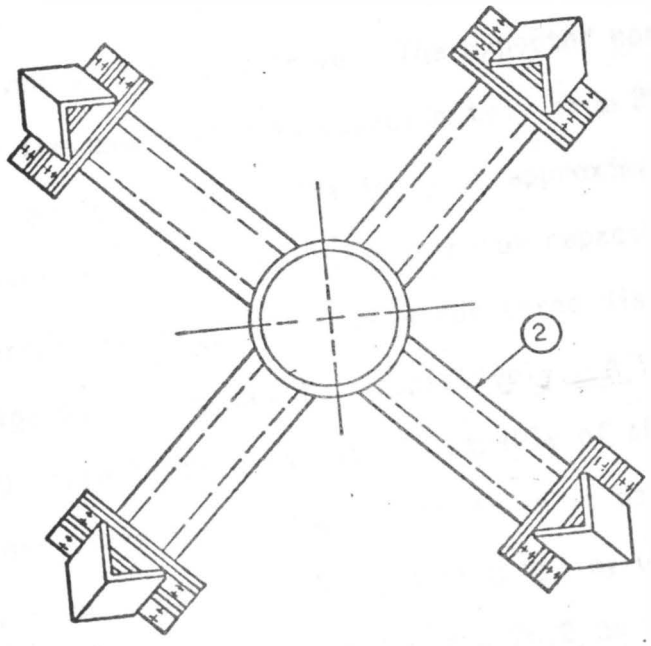

Top View

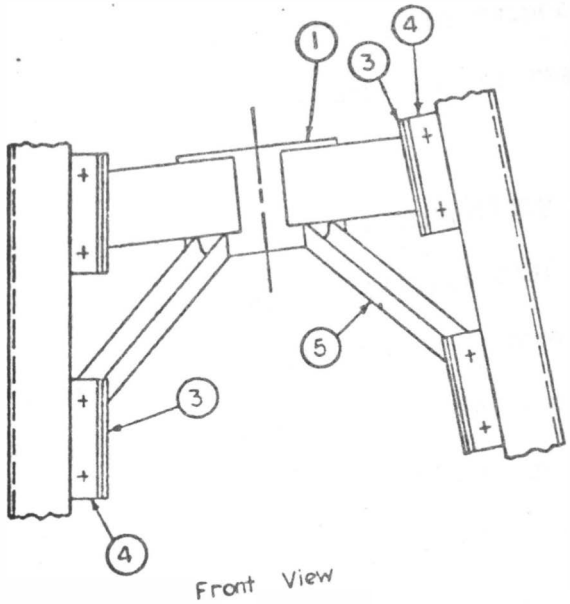

Front View

Description

1. Bearing Housing
2. Arm
3. Support plate
4. Frame plate
5. Brace

Figure 29. Turbine Upper Bearing Support

The wind energy conversion system has a two cylinder, variable speed, automotive, air conditioning, reciprocating compressor directly driven by a V-belt drive. The expected normal operating range of speed for the compressor is approximately from 2000 RPM to 3000 RPM, with the maximum volumetric efficiency at approximately 2500 RPM. The actual compressor input power, evaporator capacity, and condenser capacity versus the compressor speed for three displacements are illustrated in Figures 30, 31 and 32, respectively. A V-belt is approximately 90 percent efficient and is capable of absorbing varying torque and load vibrations. The V-belt drive is designed to transmit approximately a maximum of 4.3 kilowatts (5.8 hp) by utilizing two, B section V-belts. The V-belt drive consists of a 76.2 cm (30 in) pitch diameter large sheave mounted on the turbine rotor tube extension shaft and a 11.7 cm (4.6 in) pitch diameter small sheave mounted directly on the compressor shaft, Figure 33. By utilizing the respective pitch diameters of the sheaves, a 6.5:1 speed increase can be realized for the wind energy conversion system.

The wind turbine braking capability is provided with a 50.8 cm (20 in) diameter mechanical caliper disc brake. The brake is operated manually with a lever attachment, Figure 34. The 50.8 cm (20 in) diameter disc is mounted on the wind turbine rotor torque tube with a tapered adaptor sleeve, lock washer, and lock nut arrangement. The overall brake assembly, including the brake caliper and the lever arm, is mounted on the top of the two lower bearing assembly support arms.

The 8.3 m (27 ft) structure, that includes the rotor assembly and the tower, is secured to a steel reinforced concrete foundation with

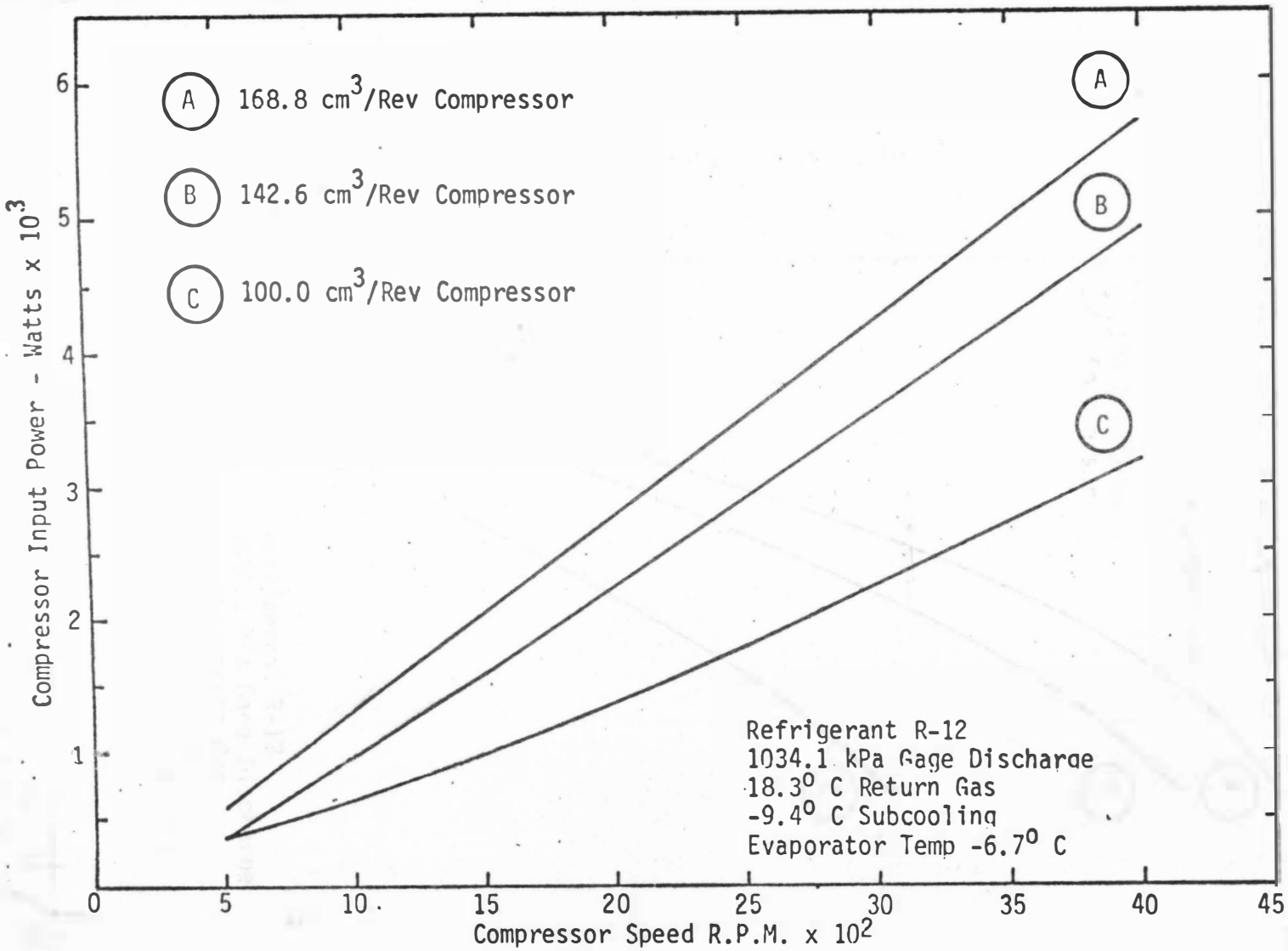

Figure 30. Power Input Curves for 168.8, 142.6 and 100.0 cm^3/Rev Reciprocating Compressors

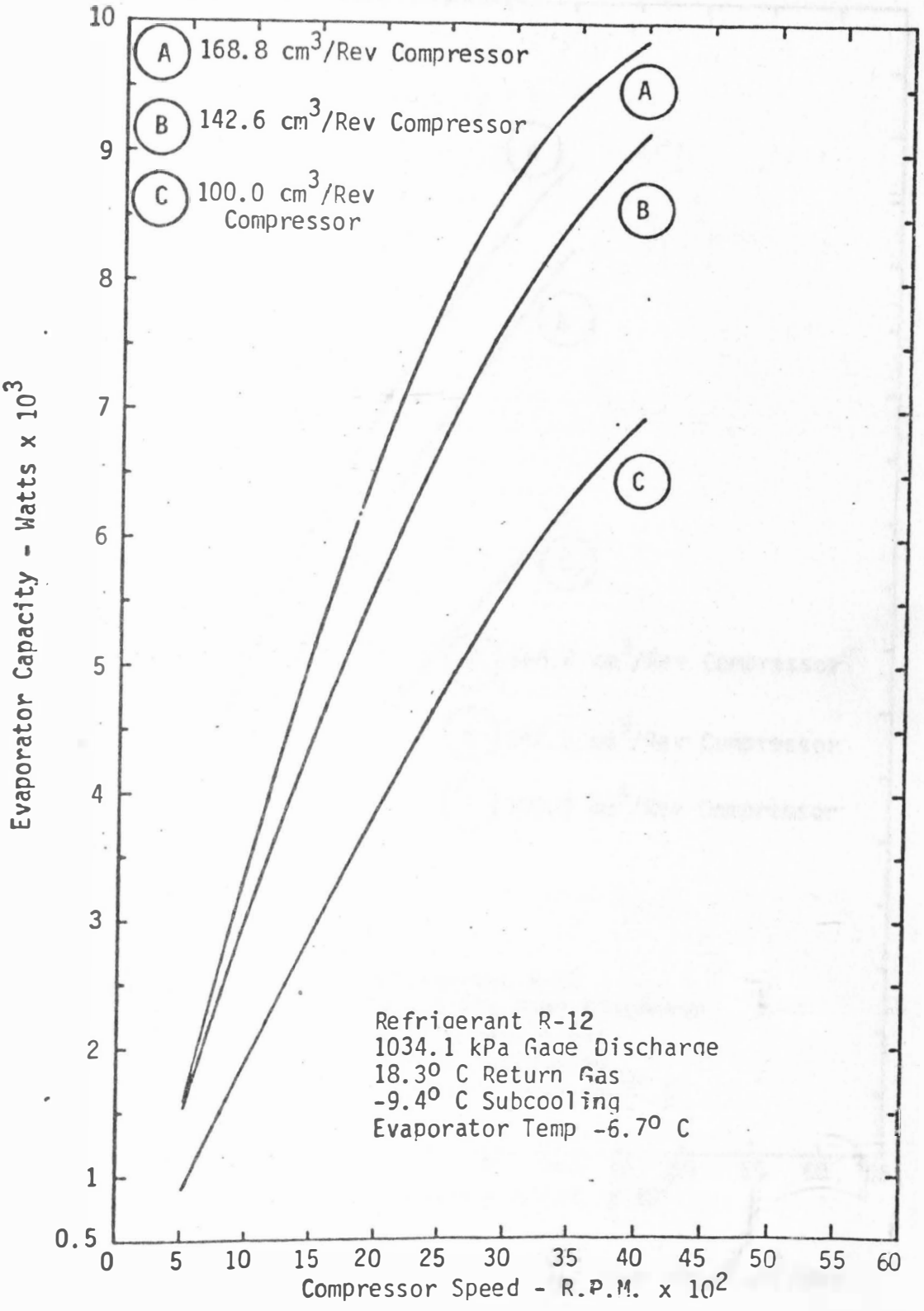

Figure 31. Evaporator Capacities for 168.8, 142.6 and 100.0 cm^3/Rev Reciprocating Compressors

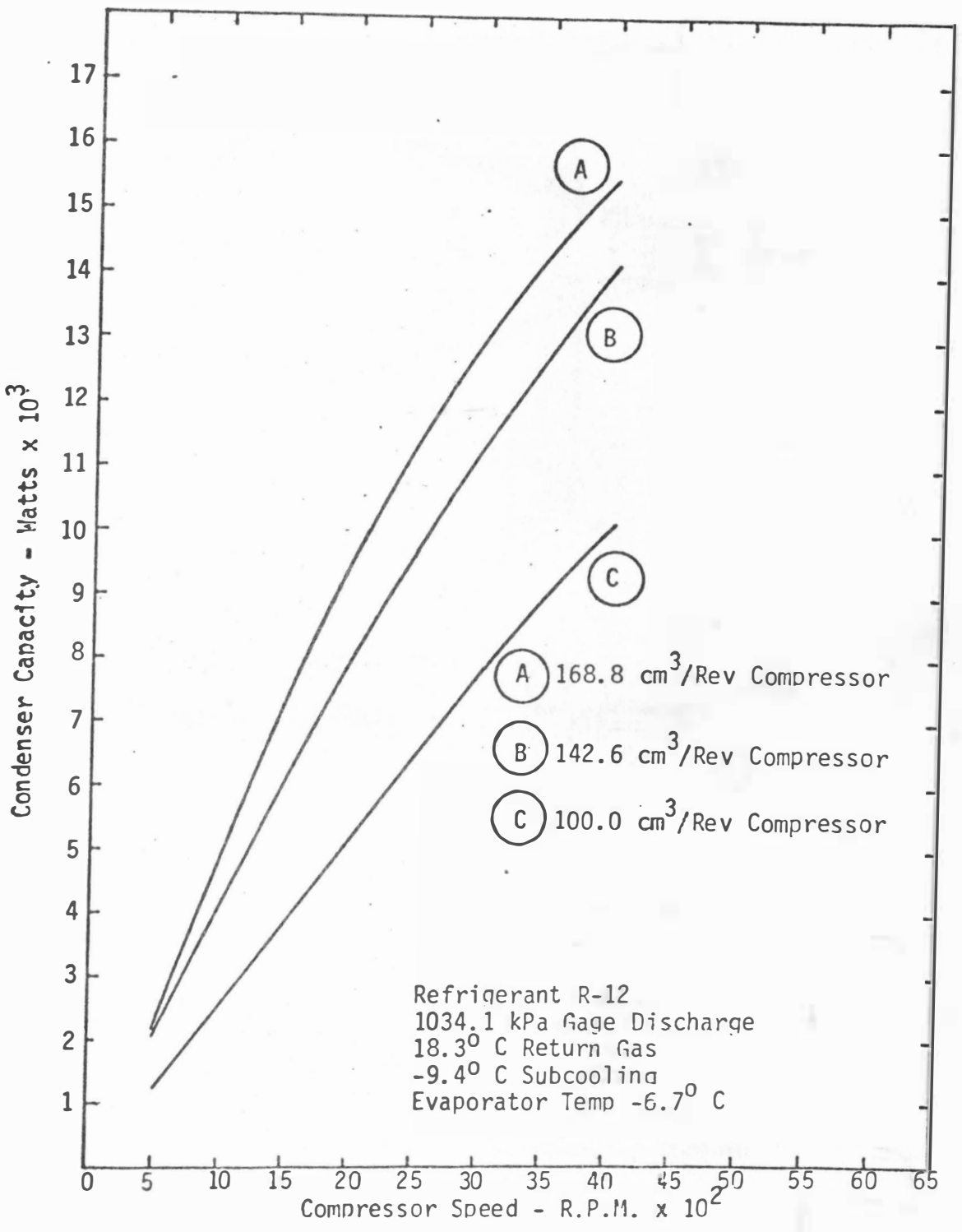

Figure 32. Condenser Capacities for 168.8, 142.6 and 100.0 cm^3/Rev Reciprocating Compressors

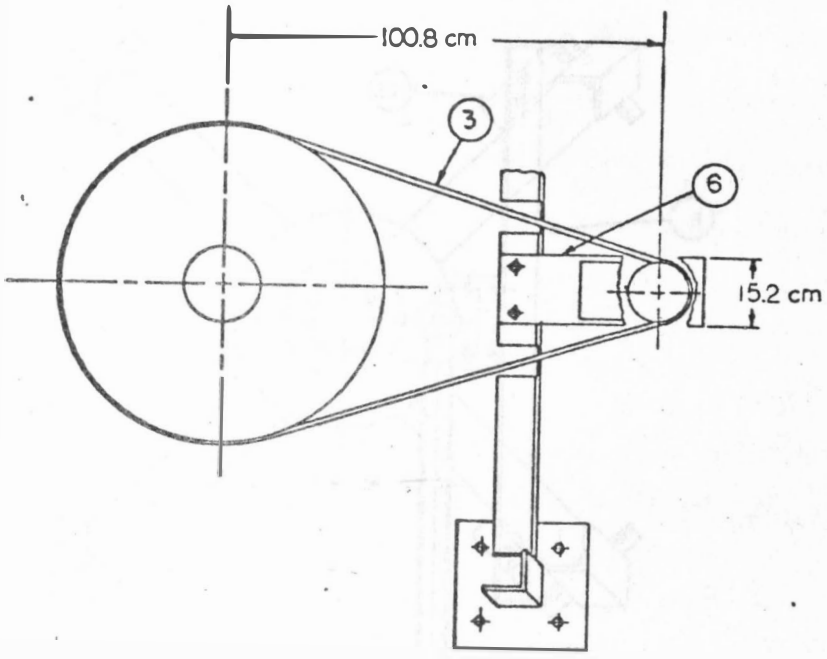

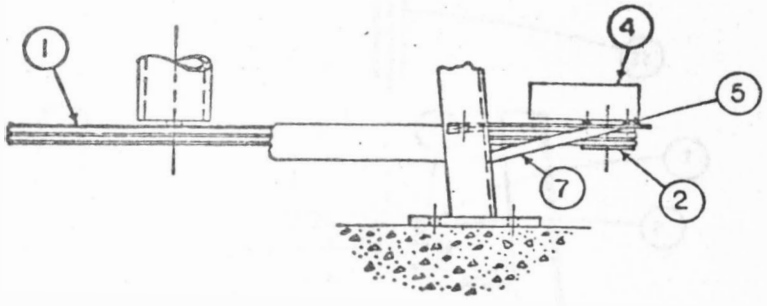

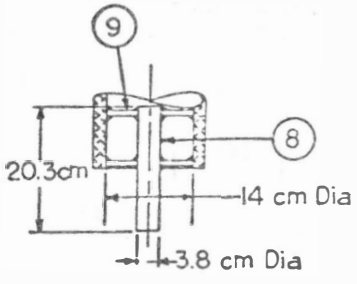

Drive Shaft Detail

Description

1. Large Sheave
2. Small Sheave
3. V-Belt
4. Air Cond Compressor
5. Vibration Isolator
6. Compressor Platform
7. Brace
8. Drive Shaft
9. Shaft Spacer

Figure 33. Turbine Drive

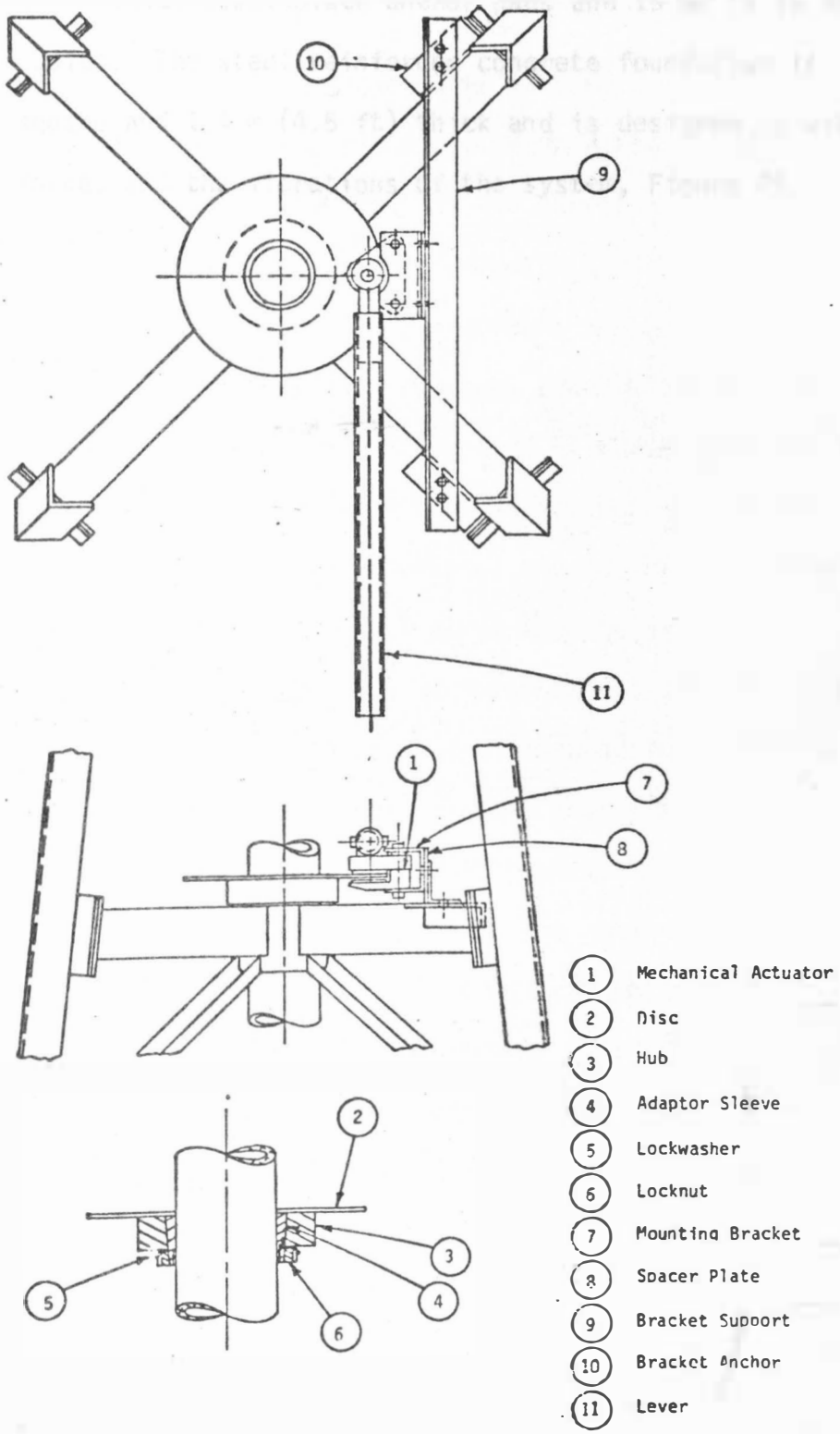

Figure 34. Caliper Disc Brake Assembly

four 19 mm (0.75 in) thick steel plate anchor pads and 19 mm (0.75 in) diameter anchor bolts. The steel reinforced concrete foundation is 2.3 m (7.5 ft) square and 1.4 m (4.5 ft) thick and is designed to withstand the wind forces and the vibrations of the system, Figure 25.

DISCUSSION AND RESULTS

Curve segments, as indicated by the curve fitting method for the proposed Savonius-Darrieus wind energy system performance curves, Figure 24, which are located to the right of the Darrieus performance constant wind velocity peaks, display more accurate curve fitting results, as compared to the existing curve segments which are located to the left of the Darrieus performance constant wind velocity peaks. This result is indicated by larger coefficient of determination, (R^2) values for the right area as compared to the coefficient of determination values for the left area. The majority of curves that were drawn for the proposed system, fitted the power curve and the straight line categories. More power curves were located intersecting the Darrieus performance curves, and the straight lines were located intersecting the existing Savonius performance curves. In the best fit areas the coefficients of determination ranged in values from 0.97 to 1.0, with the straight line fits having values of unity. The least accurate fits were noted in the transition areas which connect the Savonius curves to the Darrieus constant wind speed curves. Therefore, no attempt was made to draw the transition curve segments beyond the already existing 11.0 m/s (25 mph) constant wind speed curves as indicated in Figure 24.

The proposed wind energy conversion system, consisting of a variable speed compressor coupled to a variable speed, non-articulating Savonius rotor assisted Darrieus vertical axis wind turbine, has adequate load matching characteristics, for potential agricultural

energy applications, as noted from the projected compressor wind turbine power curve characteristics, Figure 24. For the three potential compressor displacements, a combination of B and C type loadings are applicable. Type B loadings are dominant approximately in the 4.4 m/s to 8.8 m/s (10 mph to 20 mph) wind range and type C loadings are dominant approximately from 8.8 m/s to over 15.4 m/s (20 mph to over 35 mph) wind range, indicating improved load stability for higher wind speeds, by being further away from the constant wind curve peaks.

Two sets of maximum power outputs, for the design wind speeds of cut-in, rated, and cut-out, are compared. The maximum power output consisting of selected design wind speeds at a cut-in wind speed of 5.1 m/s (11.5 mph), rated wind speed of 10.2 m/s (23 mph) and the cut-out wind speed of 15.3 m/s (34.5 mph), as obtained from the projected system power characteristic curves, is compared to the power output from a known field tested non-Savonius assisted Darrieus wind turbine having similar Darrieus parameters as the proposed system.

The power outputs, at design wind speeds of cut-in, rated, and cut-out speeds, for the proposed system, are only theoretical, in that the actual design winds for the proposed system are not known. The cut-in speed usually depends on the starting torques of the system components, such as the turbine rotor, transmission and the load. The starting torque in turn depends on the starting friction of other system components, such as bearings, compressor pistons, gears, etc. The cut-in wind speed is defined as the threshold wind velocity required to the start the system. Also, the cut-in wind speed should at least equal the average wind speed at the site. Therefore, the

cut-in wind speed for the proposed system is selected as 5.1 m/s (11.5 mph), which equals the annual average wind speed for the wind energy site at Huron, South Dakota. The rated speed is the lowest wind speed of the wind turbine at which the rated load capacity is achieved. The rated wind speed, for the proposed wind energy conversion system, is selected as 10.2 m/s (23 mph), which is twice the annual average wind speed for the wind energy site at Huron, South Dakota. The desirable compressor operating range for the proposed system, corresponding to higher volumetric efficiencies is not realized due to the specified fixed ratio speed increaser. Therefore, the rated wind speed for the proposed conditions, is not applicable for the system. The cut-out speed is the wind speed at which the turbine rotor is shut down or ceases to operate due to structural safety of the turbine and/or the load. The cut-out for the proposed wind energy conversion system is selected as 15.3 m/s (34.5 mph) which is three times the annual average wind speed for the wind energy site at Huron, South Dakota. The actual cut-out wind speed for the proposed system is unknown, because it depends on the severity of the vibrations or on the higher initial speeds of the rotor. The maximum expected turbine power output at design wind speeds, corresponding rotor speeds and compressor speeds for the two turbines are shown in Tables 1 and 2.

The projected system predicts smaller power outputs for the design wind speeds, when compared to known system power outputs at identical design wind speeds. There are several conclusions concerning these differences. Both systems have identical equatorial diameters, but the blade chord of the projected system is larger than the existing

Table 1. Maximum power output at cut-in, rated and cut-out wind speeds, corresponding rotor speeds and compressor speeds for the projected Savonius assisted Darrieus vertical axis wind turbine obtained from projected power characteristic curves.

Design Wind Speed	(m/s)	(mph)	Rotor Speed (rpm)	Compressor Speed (rpm)	Power output, kw (Hp)
Cut-in	5.1	11.5	92.0	598.0	0.5 (0.6)
Rated	10.2	23.0	178.0	1157.0	3.2 (4.3)
Cut-out	15.3	34.5	267.0	1735.5	9.7 (13.0)

Table 2. Maximum power output at cut-in, rated, and cut-out wind speeds, corresponding rotor speeds, and compressor speeds obtained from an existing non-Savonius assisted Darrieus rotor with similar Darrieus parameters to the proposed system.

Design Wind Speed	(m/s)	(mph)	Rotor Speed (rpm)	Compressor Speed (rpm)	Power output, kw (Hp)
Cut-in	5.1	11.5	107.5	699.0	0.5 (0.6)
Rated	10.2	23.0	215.0	1397.5	3.7 (5.0)
Cut-out	15.3	34.5	322.5	2096.0	10.4 (14.0)

system blade chord. The existing system total solidity is 0.2 which is smaller than the projected system solidity of 0.4. The lower solidity can shift the entire coefficient of performance curve to higher speed ratios as indicated in Figure 12, thus producing a higher power output. Also, for maximizing the power coefficient, a solidity in the range of 0.02 to 0.25 should be selected. Errors in curve projection can also influence the results of the projected power curves. The existing differences between the maximum coefficients of performance and the maximum tip speed ratios of the two systems can be ignored. These differences can be due to approximations and calculations of the above parameters, and the measurement of the maximum diameter of the turbine, or whether or not the rotor tube diameter is included in the equatorial diameter measurement. Also, the larger maximum tip speed ratios give higher power outputs. Another unknown factor, which can affect the turbine power output by increasing or decreasing the output, is the interference effect between the Savonius and Darrieus rotors.

Larger wind turbine and compressor power producing potential is not realized due to the limited power transmission capability of the V-belts, and to the selected fixed ratio speed increaser, as mentioned before. When a higher speed increaser ratio is selected, in conjunction with the existing V-belt drive, the rated capacity of the compressor can be realized. Also, higher power outputs can be obtained from the wind energy conversion system, by utilizing larger compressor displacements in conjunction with higher speed increaser ratios at higher wind speeds, Figure 24.

There exists the possibility that a three-bladed Darrieus rotor

can be self-starting, thus eliminating the need for Savonius rotors. This can be concluded from Figure 15 which depicts a three-bladed Darrieus rotor having an approximately constant torque ratio for one complete revolution of the turbine rotor.

The resonance between the blade modes and the turbine rotor can be detrimental at lower rotor speeds, Figure 23. The resonance can also be more detrimental at lower turbine rotor speeds for a variable speed system as compared to a constant speed system. Of particular concern is the need to avoid resonance crossings during rotor start-up and shut down. The resonant conditions, Figure 23, are for compound, flexible, structure blades consisting of a central curved section and coupled to two, straight blade segments. Since the proposed system has one piece blades the resonances could be shifted to higher rotor speeds. Also the exact effect of the Savonius rotors on the resonant conditions is not known, and the first critical speed and the higher critical speeds, especially in the combined turbine cut-out wind speed area are not known.

SUMMARY AND CONCLUSIONS

The utilization of energy in the agricultural sector is increasing with greater demands for production, meanwhile non-renewable fossil fuel energy is becoming more expensive and less available. Wind power offers one alternate solution for decreasing the non-renewable fuel demands for the agriculture.

Wind energy studies indicate that the Great Plains area and the East Central South Dakota have substantial amounts of energy available from the wind. A preliminary design of a vertical axis wind turbine-variable speed heat pump alternate energy system, which later can be modified to existing energy needs, is proposed that has the potential for crop drying, and space heating on East Central South Dakota farms. The wind energy conversion system consists of a cantilevered unguyed, 5 m (15 ft) diameter Savonius-Darrieus, non-articulating vertical axis wind turbine rotor, which is utilized as a prime mover for an automotive, variable speed air conditioning compressor, which is an integral part of the heat pump system.

The design wind speeds for the proposed wind energy conversion system are a cut-in speed of 5.1 m/s (11.5 mph), a rated speed of 10.2 m/s (23.0 mph) and a cut-out speed at 15.3 m/s (34.5 mph) with respective maximum rotor shaft power outputs of 0.5 kw (0.6 Hp), 3.7 kw (5.0 Hp), and 10.4 kw (14.0 Hp).

The maximum turbine shaft power outputs, at the design wind speeds, as obtained from an existing Darrieus tested wind turbine, display higher values as compared to respective power outputs which

were obtained from the Savonius-Darrieus curve that was developed. The results are appropriate, in that the Savonius-Darrieus solidity is larger than the tested Darrieus solidity. Thus the existing Darrieus power output values are selected as being representative for the proposed Savonius-Darrieus system, because both systems have identical Darrieus blade parameters.

The power outputs, at the design wind speeds for the proposed system, which are based on the cut-in wind speed of the proposed system, which equals the annual average wind speed for Huron, South Dakota, are theoretical, since the actual cut-in speed of the proposed wind turbine is unknown. Darrieus wind turbine research indicates that a three-bladed rotor can be self-starting, thus eliminating the need for Savonius Rotors. For a variable rotor speed operation in conjunction with a Darrieus rotor, Savonius rotors can be utilized to eliminate the wind gust stalling difficulty of the Darrieus rotor. The unguyed cantilevered design concept of the proposed wind energy conversion system, as compared to the guyed cable design, can minimize the resonant frequencies between the tower, guy wire, blades, and the rotor. Thus savings in materials and in costs of the system components can be realized.

SUGGESTIONS FOR FUTURE RESEARCH

A prototype of the proposed wind energy conversion system should be constructed for the evaluation of the operational and performance characteristics of the total system and its individual components.

REFERENCES

1. Ambrose, E. R. 1966. Heat Pumps and Electric Heating. John Wiley and Sons, Inc., New York, New York. Chapter 1.

2. Anonymous. 1977. Rotary A/C Compressor. Automotive Engineering, 85(2):14.

3. ASHRAE. 1978. Surface Transportation, Chapter 8, Applications Handbook.

4. ASME. 1979. Wind Turbine Energy, Mechanical Engineering, 101(6):68.

5. Banas, J. F. 1976. Economic Considerations. Proceedings of the Vertical-Axis Wind Turbine Technology Workshop, SAND 76-5586, May 17-20, Albuquerque, New Mexico 87185. pp. II-19 to II-28.

6. Banas, J. F., Kadlec, E. G. and Sullivan, W. N. 1975. Methods for Performance Evaluation of Syncronous Power Systems Utilizing the Darrieus Vertical-Axis Wind Turbine. SAND 75-0204, Sandia Laboratories, Albuquerque, New Mexico 87185.

7. Banas, J. F. and Sullivan, W. N. 1976. Engineering of Wind Energy Systems. SAND 75-0530, Sandia Laboratories, Albuquerque, New Mexico 87185.

8. Banas, J. F. and Sullivan, W. N. (Editors). 1976. Sandia Laboratories Vertical-Axis Wind Program Technical Quarterly Report October-December 1975. SAND 76-0036. Sandia Laboratories, Albuquerque, New Mexico 87185.

9. Biedermann, N. P. 1975. Wind Powered Hydrogen/Electric Systems for Farm and Rural Use. Proceedings of the Second Workshop on Wind Energy Conversion Systems, June 9-11, Washington, D.C. pp. 400-403.

10. Blackwell, B. F. 1974. The Vertical-Axis Wind Turbine "How It Works." SLA-74-0160, Sandia Laboratories, Albuquerque, New Mexico 87185.

11. Blackwell, B. F. and Feltz, L. V. 1975. Wind Energy - A Revitalized Pursuit. SAND 76-0166, Sandia Laboratories, Albuquerque, New Mexico 87185.

12. Blackwell, B. F. and Sheldahl, R. E. 1976. Selected Wind Tunnel Test Results for the Darrieus Wind Turbine. Proceedings of the Vertical-Axis Wind Turbine Technology Workshop, SAND 76-5586, May 17-20, Albuquerque, New Mexico 87185. pp. II-59 to II-72.

13. Blackwell, B. F., Sheldahl, R. E. and Feltz, L. V. 1977. Performance Data for Two- and Three-Bucket Savonius Rotors. SAND 76-0131, Sandia Laboratories, Albuquerque, New Mexico 87185.

14. Blackwell, B. F., Sheldahl, R. E. and Feltz, L. V. 1977. Wind Tunnel Performance Data for the Darrieus Wind Turbine with NACA 0012 Blades. SAND 76-0130, Sandia Laboratories, Albuquerque, New Mexico 87185.

15. Blackwell, B. F., Sullivan, W. N., Reuter, R. C. and Banas, J. F. 1977. Engineering Development Status of the Darrieus Wind Turbine. SAND 76-0650, Sandia Laboratories, Albuquerque, New Mexico 87185.

16. Chasteau, V. A. L. 1977. Operational Experience with a 5 m Darrieus Wind Turbine. Report No. 77/8. Department of Mechanical Engineering, University of Auckland, Auckland, New Zealand.

17. Cheremisinoff, N. P. 1978. Fundamentals of Wind Energy. Ann Arbor Science Publishers Inc., Ann Arbor, Michigan 48106. Chapters 4 and 5.

18. Clark, R. N. 1979. Personal Communication. Bushland, Texas 79102.

19. Clark, R. N. and Schneider, A. D. 1978. Irrigation Pumping with Wind Energy. ASAE Paper No. 78-2549, ASAE, St. Joseph, Michigan 49085.

20. Cromack, D. E. and Heronemus, W. E. 1977. Wind Power for Space Heating. Proceedings of the Third Biennial Conference and Workshop on Wind Energy Conversion Systems, September 19-21, Washington, D.C. Vol. 1. pp. 185-201.

21. Cummings, K. R. 1978. Wind Energy Application on a Dairy Farm (Abstract). Joint Meeting of the American Dairy Science Association and American Society of Animal Science, July 9-13, Michigan State University, East Lansing, Michigan.

22. Eldridge, F. R. 1975. Wind Machines. NSF Report AER-75-12937, National Science Foundation, Washington, D.C. 20550.

23. Galanis, N. and Delisle, A. 1971. Performance Evaluation of Wind Driven Heating Systems. Department of Mechanical Engineering, University of Sherbrooke, Sherbrooke, Quebec.

24. Galanis, N., Narasiah, S. and Dang, C. C. 1975. Use of Wind Energy for the Aeration of Waste Waters: A Case Study. Proceedings Second U.S. National Conference on Wind Engineering Research, June 22-25, Colorado State University, Fort Collins, Colorado.

25. Golding, E. 1955. The Generation of Electricity by Wind Power, Pitman Press, Bath, Great Britain. Chapter 2.

26. Gunkel, W. W. and Furry, R. B. 1978. Wind Energy Substitution at Dairy Milking Center Development Phase. Department of Agricultural Engineering, Cornell University, Ithaca, New York 14853.

27. Hagen, L. J. 1979. Personal Communication. United States Department of Agriculture, Agricultural Research, Kansas State University, Manhattan, Kansas 66506.

28. Hennessey, J. P., Jr. 1977. Some Aspects of Wind Power Statistics. Journal of Applied Meteorology, 16(2):119-128.

29. Holmes, J. R. 1955. Development of an Automobile Air Conditioning System. General Motors Engineering Journal, 2(3)2-9.

30. Hughes, W. L. and Dunn, C. A. 1977. Some Practical Technical and Economical Aspects of Small Wind Power Systems. Proceedings of the Third Biennial Conference and Workshop on Wind Energy Conversion Systems, September 19-21, Washington, D.C. Vol. 1. pp. 202-206.

31. Jayadev, T. S. 1976. Windmills Stage a Comeback. IEEE Spectrum, 13(11):44-49.

32. Johnson, G. L. 1978. Economic Design of Wind Electric Systems. IEEE Transactions on Power Apparatus and Systems, 97(2):554-562.

33. Justus, C. G. 1975. Annual Power Output Potential for 100-KW and 1-MW Aerogenerators. Wind Energy Conversion Systems, Second Workshop Proceedings, NSF-RAN-75-650.

34. Justus, C. G., Hargraves, W. R., Mikhail, A. and Graber, D. 1978. Methods for Estimating Wind Speed Frequency Distributions. Journal of Applied Meteorology, 17(3):350-353.

35. Kulgren, T. E., Wiedemier, D. W. and Tinsley, J. T. 1978. USAF Academy Vertical Axis Wind Turbine Development Program. Department of Civil Engineering, Engineering Mechanics and Materials, United States Air Force Academy, Colorado 80840.

36. Liljedahl, L. A. 1977. Wind Power Uses in Agriculture. Proceedings of the Third Biennial Conference and Workshop on Wind Energy Conversion Systems, September 19-21, Washington, D.C. Vol. 1. pp. 141-145.

37. Maile, L. J. H. 1976. Commercial Vertical-Axis Wind Turbine. Proceedings of the Vertical-Axis Wind Turbine Technology Workshop,

SAND 76-5586, May 17-20, Albuquerque, New Mexico 87185. pp. III-28 to III-38.

38. Newton, A. B. 1973. How to Balance Automotive Air-Conditioning Systems for Best Performance. ASHRAE Journal, 15(11):33-39.

39. Park, J. and Schwind, D. 1979. The Wind Energy Primer. Wind Power Digest, 14:6-9.

40. Ramakumar, R. 1976. Wind Driven Field Modulated Generator Systems. 11th Intersociety Energy Conversion Engineering Conference, State Line, Nevada.

41. Ramakumar, R. and Hughes, W. L. 1975. Electrical Technology Overview and Research at Oklahoma State University as Applied to Wind Energy Systems. Proceedings of the Second Workshop on Wind Energy Conversion Systems, June 9-11, Washington, D.C. pp. 265-278.

42. Reed, J. W. 1975. Wind Power Climatology. SAND 74-0435, Sandia Laboratories, Albuquerque, New Mexico 87185.

43. Reuter, R. C., Jr. 1977. Vertical Axis Wind Turbine Tie Down Design with an Example. SAND 77-1918. Sandia Laboratories, Albuquerque, New Mexico 87185.

44. Reuter, R. C. and Sheldahl, R. E. (Editors). 1976. Sandia Laboratories Vertical-Axis Wind Turbine Program Technical Quarterly Report April-June 1976. SAND 76-05181, Sandia Laboratories, Albuquerque, New Mexico 87185.

45. Savonius, S. J. 1931. The S-Rotor and Its Applications. Mechanical Engineering, 53(5):333-338.

46. Simonds, M. H. and Bodek, A. 1964. Performance Test of a Savonius Rotor Technical Report No. Tio. Brace Research Institute, McGill University, Quebec.

47. Soderholm, L. H. 1978. Using Wind Energy for Peak Electrical Load Leveling. ASAE Paper No. 78-3040, ASAE, St. Joseph, Michigan 49085.

48. South, P. and Rangi, R. S. 1971. Preliminary Tests of a High Speed Vertical-Axis Windmill Model. LTR-LA-74, National Research Council of Canada, Ottawa, Canada.

49. South, P. and Rangi, R. S. 1973. The Performance and Economics of the Vertical-Axis Wind Turbine Developed at the National Research Council, Ottawa, Canada. Report PNW 73-303, National Research Council, Ottawa, Canada.

50. Strickland, J. H. 1975. The Darrieus Turbine: A Performance Prediction Model Using Multiple Stream Tubes. SAND 75-0431, Sandia Laboratories, Albuquerque, New Mexico 87185.

51. Swift, A. H. P., Jr. 1977. Computer Aided Design of a Solar-Wind Energy System. Masters Thesis, Sever Institute of Technology, Washington University.

52. Templin, R. J. 1974. Aerodynamic Performance Theory for the NRC Vertical-Axis Wind Turbine. LTR-LA 160, National Aeronautical Establishment of the National Research Council of Canada, Ottawa, Canada.

53. Templin, R. J. and South, P. 1976. Some Design Aspects of High-Speed Vertical-Axis Wind Turbines. Paper C1. International Symposium on Wind Energy Systems, September 7-9, Cambridge, England. pp. C1-1 to C1-20.

54. Thresher, R. W. and Wilson, R. W. 1976. Design Considerations for the Darrieus Rotor. 11th Intersociety Energy Conversion Conference, State Line, Nevada. pp. 1787-1794.

55. Verma, L. 1979. Final Report on Wind Energy for Agricultural Applications. H-796. Agricultural Engineering Department, South Dakota State University, Brookings, South Dakota 57007.

56. Weingarten, L. I. and Blackwell, B. F. (Editors). 1976. Sandia Vertical-Axis Wind Turbine Program Technical Quarterly Report January-March 1976. SAND 76-0338, Sandia Laboratories, Albuquerque, New Mexico 87185.

57. Zimmer, R. P., Justus, C. G., Mason, R. M., Robinette, S. I., Sassone, P. G. and Schafer, W. A. 1975. Benefit-Cost Methodology Study with Example Application of the Use of Wind Generators. NASA CR-134864. pp. 345-349.